ADVANCED DESIGN AND OPTIMIZATION OF NOVEL FIBONACCI SWITCHED-CAPACITOR CONVERTERS FOR ULTRA-HIGH-EFFICIENCY DC-DC POWER CONVERSION

by

MANSOUR ZUBAIR HAWSAWI

A dissertation submitted in partial fulfillment of the
requirements for the degree of

DOCTOR OF PHILOSOPHY IN ELECTRICAL AND COMPUTER ENGINEERING

2025

Oakland University
Rochester, Michigan

Doctoral Advisory Committee:

Mohamed A. Zohdy, Ph.D., Chair
Amanpreet Kaur, Ph.D.
Christopher J. Kobus, Ph.D.
Suzan El Sayed, Ph.D.

To my parents, my wife Israa, son Zubair, daughter Dana, Ghadi, brothers, and sisters.

ACKNOWLEDGMENTS

I am deeply grateful to Allah Almighty for His strength, guidance, and blessings, which have been my source of support throughout the completion of this dissertation. My sincere appreciation goes to my advisor, Dr. Mohamed A. Zohdy, whose invaluable guidance, unwavering support, and insightful contributions have been essential to my Ph.D. journey. His profound expertise and encouragement have played a crucial role in the development of my research.

I would also like to express my heartfelt thanks to my dissertation committee members, Dr. Amanpreet Kaur, Dr. Christopher Kobus, and Dr. Suzan El Sayed, for their constructive feedback and continuous encouragement. Their contributions have greatly enhanced the quality of this work.

Additionally, I am profoundly grateful to my family, especially my wife Israa, my older son Zubair, my daughters Dana and Ghadi, and my brothers and sisters, for their unwavering support, love, and encouragement throughout this journey. I also dedicate this work to the soul of my late father, whose memory and spirit have always been a source of inspiration.

Lastly, I extend my thanks to everyone who supported and inspired me throughout my Ph.D. studies at Oakland University, whether through kind words, smiles, or acts of encouragement. Your support has made this journey possible.

Mansour Zubair Hawsawi

ABSTRACT

ADVANCED DESIGN AND OPTIMIZATION OF NOVEL FIBONACCI SWITCHED-CAPACITOR CONVERTERS FOR ULTRA-HIGH-EFFICIENCY DC-DC POWER CONVERSION

by

MANSOUR ZUBAIR HAWSAWI

Adviser: Mohamed A. Zohdy, Ph.D.

The study explores the design and analysis of two DC-DC converter configurations integrated with solar photovoltaic (PV) renewable energy systems, comparing the conventional boost converter with a novel Fibonacci switched-capacitor (FSC) boost converter. Advanced Maximum Power Point Tracking (MPPT) algorithms, including Perturb and Observe (P&O), Incremental Conductance (INC), Genetic Algorithm (GA), and Particle Swarm Optimization (PSO), are paired with both converters to optimize energy extraction from solar PV systems. Simulation results reveal that both converter topologies, when combined with the appropriate MPPT algorithms, effectively maximize power output from the solar PV system.

The FSC converter demonstrates exceptional performance, particularly in terms of current handling and voltage regulations. Featuring a modular arrangement of capacitors and MOSFETs synchronized by the CD4007 IC, the FSC converter adapts efficiently to dynamic load changes and varying irradiance conditions, resulting in enhanced current control, minimized output voltage fluctuations, and improved voltage regulation. Integrated with the GA-MPPT algorithm, the FSC converter achieves a significant boost in output current, reaching up to 70 A compared to just 10 A for the conventional boost

converter. Furthermore, the FSC design excels in reducing electromagnetic interference (EMI) and simplifies thermal management, making it an ideal solution for high-efficiency applications.

Both converter topologies are validated through MATLAB/Simulink simulations and hardware implementations. The hardware prototype, incorporating IRF540 MOSFETs and 22 μF capacitors, shows the scalability, compactness, and reliability of the FSC converter. The findings highlight the potential of the FSC converter in renewable energy systems, automotive applications, portable electronics, and other high-efficiency, compact systems. It positions the FSC topology as a promising alternative to traditional inductor-based designs, offering an innovative solution to address performance limitations in renewable energy conversion.

TABLE OF CONTENTS

TABLE OF CONTENTS- (continued)

TABLE OF CONTENTS- (continued)

LIST OF TABLES

LIST OF FIGURES

LIST OF FIGURES- (continued)

LIST OF ABBREVIATIONS AND SYMBOLS

PV	Solar photovoltaic
MPPT	Maximum Power Point Tracking
P&O	Perturb and Observe
INC	Incremental Conductance
PSO	Particle Swarm Optimization
GA	Genetic Algorithms
SC	Switched Capacitor
I-V	Current - Voltage
P-V	Power - Voltage
MPP	Maximum Power Point
ΔP	Change in Power
ΔV	Change in Voltage
dP/dV	Derivative of Power with the Voltage
dI/dV	Derivative of Current with the Voltage
PCB	Printed Circuit Board Learning Machine Algorithm
EMI	Electromagnetic Interference
GaN	Gallium Nitride
FSSC	Fibonacci Sequence Switched Capacitor
KCL	Kirchhoff’s Current Law

KVL	Kirchhoff’s Voltage Law
CCM	Continuous Conduction Mode
FSSC	Fibonacci Sequence Switched Capacitor
KCL	Kirchhoff’s Current Law
KVL	Kirchhoff’s Voltage Law
CCM	Continuous Conduction Mode
FSSC	Fibonacci Sequence Switched Capacitor
KCL	Kirchhoff’s Current Law
KVL	Kirchhoff’s Voltage Law
CCM	Continuous Conduction Mode
FSSC	Fibonacci Sequence Switched Capacitor
KCL	Kirchhoff’s Current Law
KVL	Kirchhoff’s Voltage Law
CCM	Continuous Conduction Mode
FSSC	Fibonacci Sequence Switched Capacitor
KCL	Kirchhoff’s Current Law

LIST OF ABBREVIATIONS AND SYMBOLS- (continued)

KVL	Kirchhoff’s Voltage Law
DCM	Discontinuous Conduction Mode
N_P	Parallel Strings
N_s	Series Connected Modules Per String
C	Capacitor
R_L	Load Resistance
FG	Function Generator
FC	Fibonacci Converter
CE	Cost Efficiency
SS	Steady State

CHAPER ONE

INTRODUCTION

The field of renewable energy, particularly solar photovoltaic (PV) systems, has seen significant advancements in recent years[1]. DC-DC converters play a vital role in enhancing the performance of solar photovoltaic (PV) systems by optimizing energy extraction through advanced Maximum Power Point Tracking (MPPT) techniques[2]. These converters dynamically regulate the power flow, ensuring efficient harvesting of solar energy while maintaining voltage stability and improving overall system efficiency[3]. Their integration with sophisticated MPPT algorithms enables precise tracking of the maximum power point, maximizing the energy yield from solar PV systems[4]. This dissertation presents a comparative analysis of conventional boost converters and switched-capacitor boost converters, highlighting their roles in enhancing the performance of solar photovoltaic (PV) systems. Special emphasis is placed on the Fibonacci switched-capacitor topology, with a focus on optimizing circuit design to achieve superior efficiency and performance. Furthermore, the study explores the implementation of the improved circuit in both software and hardware, ensuring its practicality and effectiveness in real-world applications.

1.1 Literature Review

DC-DC converters and MPPT techniques have undergone extensive research. Early works focused on traditional boost converters due to their simplicity and effectiveness in basic power conversion tasks[5]. Laid the foundation for MPPT algorithms by introducing the Perturb and Observe (P&O) method, which has since been widely applied to solar PV systems. However, despite its popularity, P&O has limitations in dynamic conditions, leading to inefficiencies in power extraction.

Laid the foundation for MPPT algorithms by introducing the Perturb and Observe (P&O) method, which has since been widely applied to solar PV systems. However, despite its popularity, P&O has limitations in dynamic conditions, leading to inefficiencies in power extraction.

Incremental Conductance (INC) emerged to address these limitations, offering more accurate MPP tracking under changing irradiance levels, as described by[6]. More recently, metaheuristic algorithms like Particle Swarm Optimization (PSO) and Genetic Algorithms (GA) have been introduced to improve MPPT efficiency. Studies by [7] demonstrate that these techniques offer superior performance compared to traditional methods.

In addition, switched capacitor converters have attracted increasing interest due to their ability to achieve higher voltage gains without the need for inductors, demonstrated that switched capacitor converters combined with advanced MPPT algorithms can outperform conventional boost converters in solar PV systems[8].

Research on Fibonacci switched-capacitor (FSC) converters has advanced significantly, with several studies focusing on improving their performance and efficiency. One study explores a high voltage gain switched-capacitor DC-DC converter utilizing three parallel-connected Fibonacci converters, demonstrating enhanced efficiency and reduced voltage stress[9]. Another research effort presents a monolithic voltage-scalable FSC converter with an intrinsic charge recycling technique, aimed at minimizing parasitic charge losses and improving overall energy conversion efficiency[10]. Furthermore, the general analysis of Fibonacci charge pump SSL output characteristics provides a theoretical derivation of an analytical model that incorporates bottom-plate and closed-switch parasitic capacitances, offering valuable insights into circuit non-idealities[11]. Additionally, a multiphase Fibonacci switched-capacitor converter is analyzed using a novel Switched Fibonacci Number (SFN) representation and algebraic modeling, with experimental validation confirming its effectiveness[12]. In addition, a practical design strategy for a two-phase step-up FSC converter introduces two novel gate-driving techniques designed to simplify circuit complexity and enhance converter reliability[13],[14].

In parallel, DC-DC boost converter technologies have also evolved to address challenges related to efficiency, power density, and voltage gain. A high-efficiency soft-switched boost converter has been investigated for renewable energy applications, integrating zero-voltage switching (ZVS) and zero-current switching (ZCS) techniques to reduce switching losses and improve overall efficiency[15], [16]. Another study focuses on an interleaved boost converter with coupled inductors, demonstrating enhanced power density and reduced current ripple[17]. Moreover, a high step-up DC-DC converter incorporating a voltage multiplier and coupled inductor has been introduced to achieve ultra-high voltage gain with minimal switching losses[18]. A non-isolated quadratic boost converter has also been developed, providing a significantly high voltage gain suitable for fuel cell and battery-powered applications[19]. Lastly, a hybrid switched-capacitor and inductor-based boost converter combines the advantages of both technologies to optimize efficiency and reduce component stress, making it a promising approach for high-performance power conversion[20], [21].

1.2 Motivation and Research Goal

The primary motivation for this research is the need to enhance solar PV system efficiency by improving the performance of DC-DC converters and MPPT algorithms. Traditional boost converters have certain limitations, particularly in handling dynamic environmental conditions. This dissertation aims to explore switched capacitor converters as a potential solution, comparing them with conventional boost converters to determine their suitability for solar PV applications.

1.3 Dissertation Contributions

This dissertation makes several contributions to the field of solar energy and power electronics:

- A comprehensive comparative analysis between conventional boost converters and switched capacitor boost converters.
- An evaluation of the effectiveness of various MPPT algorithms (P&O, INC, PSO, GA) in enhancing the performance of these converters.
- The application of the Genetic Algorithm (GA) with MPPT enhances the FSC converter's performance, significantly improving the output voltage profile and providing better current control and voltage regulation.
- The introduction of a novel Fibonacci sequence design for switched capacitor converters.
- Performance evaluation of both converter types using MATLAB/Simulink

simulations under dynamic conditions.

1.4 Overview of Renewable Energy Systems

In recent years, renewable energy has emerged as a critical solution for addressing the environmental and economic challenges posed by conventional energy sources. The increasing concerns about greenhouse gas emissions, resource depletion, and the long-term sustainability of fossil fuels have driven both policymakers and industries to explore cleaner and more sustainable alternatives[22]. As a result, solar energy has become one of the most widely adopted and rapidly growing renewable energy sources worldwide, contributing to the global shift towards sustainable energy systems[23].

The core technology driving solar energy adoption is the photovoltaic (PV) system, which converts sunlight directly into electricity through the photovoltaic effect[24]. PV systems are not only scalable but also versatile, making them suitable for a wide range of applications, from small residential installations to large utility-scale solar farms[25]. The increasing efficiency of photovoltaic cells, along with the declining costs of PV technology, has accelerated the deployment of solar energy systems across the globe[22]. Moreover, the integration of PV systems with grid networks and the development of storage solutions have further enhanced the feasibility and reliability of solar energy as a primary energy source[25].

Despite these advancements, photovoltaic systems are inherently variable due to their dependence on environmental factors such as irradiance (the intensity of sunlight) and temperature[24]. Solar irradiance can fluctuate throughout the day due to cloud cover, shading, or changes in the sun's position, while temperature variations can impact the efficiency of PV cells[25]. These fluctuations pose significant challenges in maintaining a consistent power output, which is crucial for reliable energy generation and grid stability. As solar PV systems continue to expand, the need for optimizing energy conversion and ensuring system efficiency becomes even more critical[26].

To address these challenges, the role of power electronics, specifically DC-DC converters, has become essential in the integration of solar PV systems[27]. DC-DC converters are responsible for regulating the voltage and current from the solar panels to match the load or grid requirements, ensuring that the system operates efficiently under varying environmental conditions. These converters not only step up or step down the voltage as needed but also help in reducing power losses, thereby improving the overall energy yield of the PV system.

Additionally, Maximum Power Point Tracking (MPPT) algorithms play a vital role in enhancing the performance of solar PV systems by dynamically adjusting the operating point of the PV array to ensure maximum power extraction. MPPT techniques continuously monitor the output of the solar panels and adjust the load to ensure that the system operates at its optimal power point, even when environmental conditions are not ideal. This capability is especially important in large-scale PV systems, where even small efficiency improvements can result in significant increases in overall power output. Various MPPT algorithms, ranging from traditional methods like Perturb and Observe (P&O) and Incremental Conductance (INC) to more advanced techniques such as Particle Swarm Optimization (PSO) and Genetic Algorithms (GA), have been developed to enhance the efficiency of solar PV systems under dynamic conditions.

1.5 Role of DC-DC Converters in Solar PV Systems

DC-DC converters are pivotal components in the integration and operation of solar photovoltaic (PV) systems[28]. Their primary function is to regulate and optimize the voltage and current produced by solar panels to ensure that the maximum possible power is transferred from the PV array to the load or the grid[29]. Given the fluctuating nature of solar energy, caused by factors such as varying irradiance and temperature, the role of DC-DC converters becomes even more critical in maintaining system stability and efficiency[30]. The precise control and power management provided by these converters enable solar PV systems to function effectively across a wide range of environmental conditions, thereby enhancing both the reliability and the efficiency of solar energy harvesting.

At the heart of this regulatory process is the ability of DC-DC converters to match the PV system's output to the load or grid requirements by stepping up or stepping down the voltage as necessary[31]. This process is essential because the voltage output from solar panels can vary significantly depending on environmental conditions. For instance, during periods of low irradiance, such as cloudy days or early mornings, the voltage output from the solar array may be insufficient for the system's load requirements, necessitating a step-up conversion. Conversely, during periods of high irradiance, the voltage may need to be stepped down to protect the load or the inverter from overvoltage conditions[32]. Without efficient DC-DC conversion, much of the energy produced by solar PV systems would be lost, especially during suboptimal operating conditions, leading to reduced overall system efficiency[33].

Traditionally, the conventional boost converter has been the most commonly used topology in solar PV systems for stepping up the voltage from the solar array to a higher level that is suitable for grid or load integration[3],[34]. This converter topology is simple, reliable, and cost-effective, making it widely applicable in residential and small-scale solar installations[35]. However, conventional boost converters exhibit several limitations, particularly in dynamic environments where the input voltage fluctuates rapidly due to changes in sunlight exposure[36]. Under such conditions, conventional boost converters may experience significant efficiency losses due to their reliance on inductors[37], which can lead to slow response times, higher power losses, and reduced voltage regulation accuracy.

One of the key limitations of conventional boost converters is their inefficiency in handling high power levels. The inductor used in these converters tends to saturate at high currents, leading to increased power dissipation and heat generation[38]. This not only affects the overall system efficiency but also limits the scalability of the converter for larger solar PV systems. As a result, conventional boost converters are often less suited for large-scale solar farms or environments where the solar irradiance fluctuates rapidly, such as in regions prone to partial shading or where there are frequent transitions between cloudy and sunny conditions.

In response to these challenges, alternative DC-DC converter topologies have been developed to improve the efficiency and performance of solar PV systems under dynamic conditions[39]. One promising solution is the switched capacitor (SC) converter. Unlike conventional boost converters, which rely heavily on inductors for energy storage and transfer, switched capacitor converters use capacitors and switches to step up or step-down voltage. This allows for a more compact and efficient design, particularly in applications where high voltage gains are required without the drawbacks of inductor-based energy transfer.

Switched capacitor converters offer several advantages over conventional boost converters. First, they eliminate the need for bulky and lossy inductors, which reduces the overall size, weight, and cost of the system[40]. This makes SC converters particularly attractive for applications where space is a constraint, such as in rooftop solar installations or portable solar power systems. Second, SC converters can achieve higher voltage gains compared to conventional boost converters, making them more efficient in scenarios where large voltage step-ups are required. This is especially relevant in grid-tied solar systems, where the output voltage from the solar array often needs to be significantly higher than the input voltage to meet grid requirements.

Moreover, switched capacitor converters have been shown to perform better under rapidly changing environmental conditions, offering faster response times and better voltage regulation than their conventional counterparts. Studies have demonstrated that SC converters can more effectively handle the dynamic nature of solar energy, providing greater stability and efficiency in systems where irradiance levels fluctuate frequently throughout the day[41]. This improved performance is particularly important in maximizing the energy yield of solar PV systems, as it allows the system to extract more power from the solar array even under suboptimal conditions.

Despite the advantages of switched capacitor converters, their adoption of large-scale solar PV systems is still in the early stages. One of the challenges associated with SC converters is their complexity in terms of control and switching schemes. The increased number of switches and capacitors required in SC topologies can complicate the design and control strategy, particularly when scaling up for larger systems[42]. However, advancements in digital control and power electronics have made it possible to mitigate these challenges, and ongoing research continues to improve the scalability and performance of switched capacitor converters for solar applications.

1.6 Fundamental and Background of PID controller

A Proportional Integral Derivative (PID) controller is a widely used control loop feedback mechanism in industrial control systems. It is employed to regulate processes such as temperature, pressure, flow, speed, and other variables. The PID controller continuously calculates an error value as the difference between a desired setpoint (SP) and a measured process variable, and applies a correction based on proportional, integral, and derivative terms[43].

1.6.1: The PID controller consists of three main components:

1.6.1.1: Proportional (P) Term:

- The proportional term produces an output that is proportional to the current error value.
- The proportional gain (K_p) determines the strength of the response to the error.

Formula: P = $K_p \times$ e(t) (1.1)

Where:

e (t) is error at time t

- Effect: Reduces the error but may not eliminate it completely, leading to a steady-state error.

1.6.1.2: Integral (I) Term:

- The integral term accounts for the accumulation of past errors over time.
- It helps eliminate steady-state errors by integrating the error over time.
- The integral gain (K_I) determines the weight of past errors
- Formula: $I = K_i \times \int_0^t e(t) \times dt$ (1.2)
- Effect: Eliminates residual steady-state errors but can cause overshoot if not tuned properly.

1.6.1.3: Derivative (D) Term:

- The derivative term predicts future error based on the rate of change of the error.
- It dampens the system response and reduces overshoot.
- The derivative gain (K_d) determines the sensitivity to the rate of change.
- Formula: $D = K_d \times \frac{d\,e(t)}{dt}$ (1.3)
- Effect: Improves stability and reduces oscillations.

1.6.2: Mathematical Representation of the PID Controller

The PID (Proportional Integral Derivative) controller is a classical control technique used to regulate system outputs by minimizing errors. The general mathematical equation for a PID controller is[44]:

$$\mathrm{Out(t)} = \mathrm{P} = \mathrm{K_p} \times \mathrm{e(t)} + K_i \times \int_0^t e(t) \times dt + K_d \times \frac{d\, e(t)}{dt} \tag{1.4}$$

1.6.3: Background and History

- The PID controller was first developed in the early 20th century for industrial automation[45].
- It became widely adopted due to its simplicity, effectiveness, and adaptability to a wide range of systems.
- The Ziegler-Nichols method, introduced in the 1940s, provided a systematic way to tune PID controllers[46].

1.6.4: Advantages of PID Controllers

- Simple structure and easy to implement.
- Effective for a wide range of systems.
- Can be tuned to achieve precise control.

1.6.5: Limitations of PID Controllers

- May not perform well for highly nonlinear or complex systems.
- Requires careful tuning to avoid instability or oscillations.
- Sensitive to noise in the derivative term.

CHAPTER TWO

MAXIMUM POWER POINT TRACKING TECHNIQUES

Maximum Power Point Tracking (MPPT) algorithms play a vital role in enhancing the efficiency of solar photovoltaic (PV) systems by ensuring that the system operates at its maximum power point (MPP) under varying environmental conditions. The ability of MPPT algorithms to dynamically adjust the operating parameters of the PV array, in response to changes in irradiance, temperature, and shading, is crucial for maximizing the energy output of the system[47]. As solar PV systems are inherently variable due to their dependence on sunlight, MPPT techniques allow for the real-time optimization of the energy harvested from the solar panels. This chapter provides a comprehensive analysis of the various MPPT algorithms, their respective strengths and weaknesses, and their applicability to different DC-DC converter topologies used in solar energy systems. MPPT algorithms are essential for optimizing the power output of solar PV systems[48].

2.1 Overview of MPPT Techniques

Maximum Power Point Tracking (MPPT) techniques are integral to the efficient operation of solar photovoltaic (PV) systems. Their primary function is to ensure that the PV system continuously operates at its Maximum Power Point (MPP), the point where the solar panels produce the maximum possible power output under given environmental conditions[49]. Achieving this requires dynamic adjustments to the system's operating parameters, as the MPP varies with changes in environmental factors such as solar irradiance, temperature, and shading[50]. The ability of MPPT algorithms to optimize power extraction from the PV array, regardless of fluctuating environmental conditions, is essential for improving the overall efficiency and energy yield of solar PV systems[51].

The need for MPPT arises from the non-linear current-voltage (I-V) and power-voltage (P-V) characteristics of solar cells[52]. The power generated by a PV module depends on both the voltage and current, which are directly influenced by environmental conditions. As the irradiance and temperature change throughout the day, the MPP shifts along the P-V curve. Without a proper MPPT technique, a PV system would operate inefficiently, either below or above the MPP, leading to significant energy losses. MPPT algorithms, therefore, serve the critical function of tracking and adjusting the operating point to ensure that the system remains at or near the MPP, thereby maximizing the energy harvested from the solar array[53].

Over the years, numerous MPPT techniques have been developed and refined, ranging from simple, heuristic methods to more sophisticated, algorithm-based approaches. These techniques vary in terms of complexity, response speed, tracking accuracy, and implementation costs, making them suitable for different applications depending on the size and requirements of the PV system. Among the most used MPPT techniques are Perturb and Observe (P&O), Incremental Conductance (INC), and more advanced metaheuristic algorithms such as Particle Swarm Optimization (PSO) and Genetic Algorithms (GA).

2.2 Perturb and Observe (P&O) Algorithm

The Perturb and Observe (P&O) algorithm is one of the simplest and most widely used MPPT techniques due to its ease of implementation and low computational requirements. The fundamental concept behind the P&O method is to periodically perturb the operating voltage of the PV array and observe the resulting change in power output. If the power increases after the perturbation, the system continues to adjust the operating voltage in the same direction; if the power decreases, the perturbation direction is reversed. This iterative process allows the system to track the MPP by continuously adjusting the voltage and moving towards the point of maximum power[54].

While the P&O algorithm is effective in stable environmental conditions, its performance is limited under rapidly changing irradiance or temperature[55]. The algorithm tends to oscillate around the MPP, leading to energy losses during steady-state operation[56]. Furthermore, under conditions where the MPP shifts rapidly (e.g., due to passing clouds or shading), the P&O method may fail to accurately track the new MPP, resulting in suboptimal power extraction. Despite these limitations, P&O remains popular for small-scale and cost-sensitive PV applications, particularly where the simplicity of the algorithm outweighs the need for high tracking accuracy.

The P&O algorithm is one of the earliest and most widely used MPPT techniques due to its simplicity. It works by periodically perturbing the system's operating point and observing changes in power output. While effective in stable conditions, P&O suffers from power losses due to oscillations around the MPP under fluctuating environmental conditions[57].

The Perturb and Observe (P&O) Algorithm operates based on the iterative adjustment of the operating voltage of a solar PV array to track the Maximum Power Point (MPP). This process involves perturbing (changing) the operating voltage and observing the resulting change in power output. The basic equations governing the P&O algorithm are focused on the relationship between voltage, current, and power in a PV system. Here are the key equations and principles used in the P&O algorithm:

1- Power Calculation: The power output of the PV module is calculated at each perturbation step:

$$P = V \times I \tag{2.1}$$

Where:

- P is the power output of the PV array.
- V is the voltage across the PV array.
- I is the current output of the PV array

2- Perturbation and Observation: The core of the P&O algorithm involves perturbing the voltage of the PV module and observing the change in power. The following conditions are evaluated to determine the next step:

- If the change in power ΔP with respect to the change in voltage ΔV is positive:

$$\Delta P = Pnew - Pold > 0 \; and \; \Delta V = Vnew - Vold > 0 \tag{2.2}$$

It means that increasing the voltage moves the operating point closer to the MPP, so the perturbation should continue in the same direction (increase the voltage).

- If the change in power ΔP is negative:

$$\Delta P = Pnew - Pold < 0 \; and \; \Delta V = Vnew - Vold < 0 \tag{2.3}$$

It indicates that the perturbation has moved the operating point away from the MPP, so the perturbation direction should be reversed (decrease the voltage).

3- Direction of Adjustment: The P&O algorithm adjusts the voltage in the following way based on the sign of ΔP:

- If $\frac{\Delta P}{\Delta V} > 0$ (2.4)

Increase voltage to move closer to the MPP.

- If $\frac{\Delta P}{\Delta V} < 0$ (2.5)

Decrease voltage to return towards the MPP.

4- Step Size Adjustment: The step size ΔV determines how much the voltage is perturbed during each iteration:

$$Vnew = Vold + \Delta V \quad (2.6)$$

The step size ΔV affects the speed of convergence to the MPP. A larger ΔV results in faster tracking but may cause larger oscillations around the MPP, while a smaller ΔV results in more precise tracking but slower response times. Here is the flow chart for P&O algorithm.

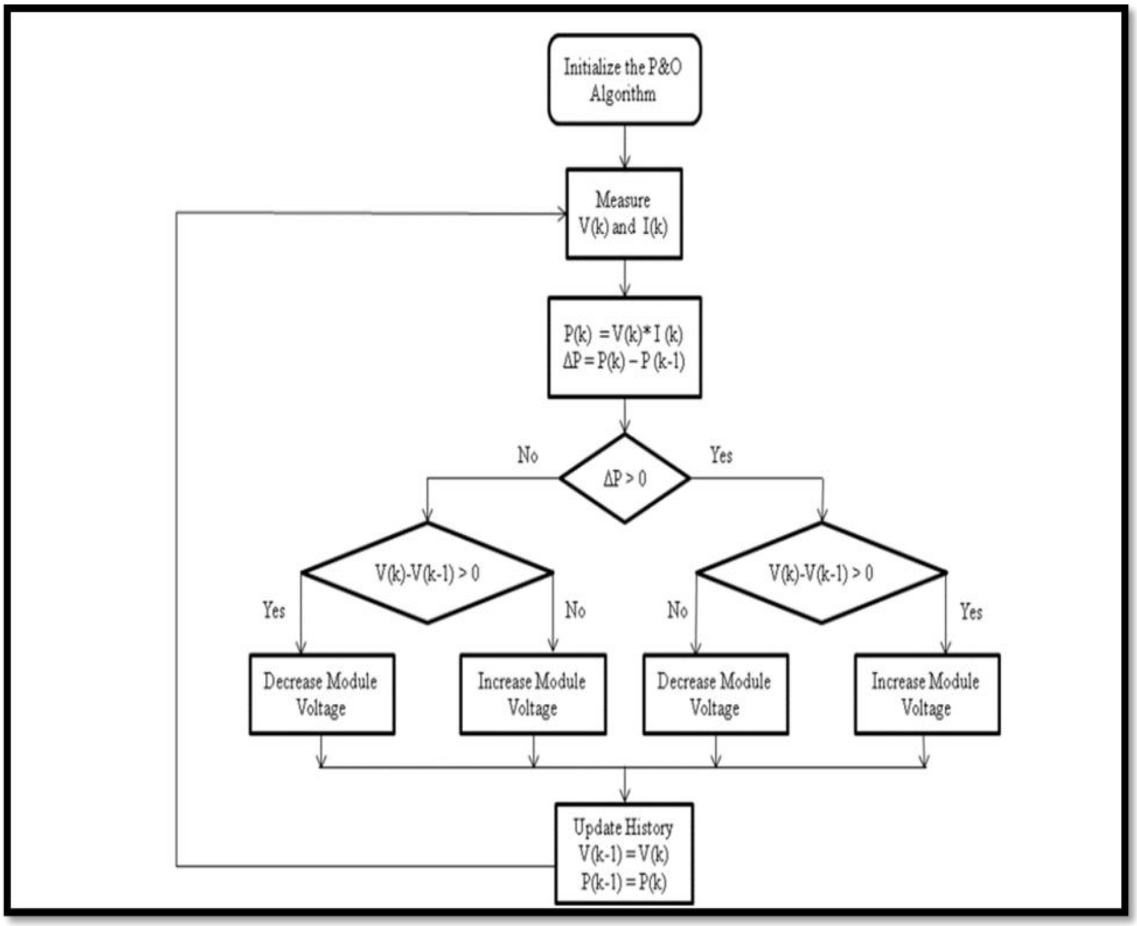

Figure 2.1 Perturbation and Observation Algorithm[58]

2.2.1 Strengths:

The primary advantage of the P&O algorithm is its simplicity. It requires minimal computational resources, making it ideal for cost-sensitive applications and small-scale solar PV systems where processing power and hardware complexity are limited. Additionally, P&O is relatively easy to implement, and its real-time operation makes it effective in basic MPPT tasks under stable environmental conditions.

2.2.2 Weaknesses:

However, the P&O method has notable limitations, particularly in dynamic environments where irradiance and temperature change rapidly. The algorithm tends to oscillate around the MPP, leading to power losses during steady-state operation. Moreover, when environmental conditions change rapidly, such as during partial shading or cloudy conditions, the P&O algorithm may fail to accurately track the MPP, resulting in suboptimal power extraction[59]. These oscillations and tracking inaccuracies reduce the overall efficiency of the system, especially in large-scale or grid-connected solar PV installations.

2.3 Incremental Conductance (INC) Algorithm

The INC algorithm addresses some of the shortcomings of P&O by using the derivative of the power with respect to the voltage to track the MPP more accurately. It performs better under rapidly changing irradiance levels but is more complex to implement[60].

The Incremental Conductance (INC) algorithm was developed to address some of the limitations associated with the P&O method, particularly its inability to accurately track the MPP under dynamic conditions. The INC technique is based on the derivative of the power with respect to the voltage is zero (dP/dV = 0). By continuously measuring the incremental conductance (dI/dV) and comparing it to the instantaneous conductance (I/V), the INC algorithm can determine whether the operating point is to the left or right of the MPP and adjust the voltage accordingly.

$$\frac{dPpv}{dVpv} = 0 \tag{2.7}$$

$$\frac{dPpv}{dVpv} = \frac{dIpv\; dVpv}{dVpv} + \frac{dVpv\; dIpv}{dVpv} \tag{2.8}$$

$$\frac{dIpv}{dVpv} = -\frac{Ipv}{Vpv} \tag{2.9}$$

The algorithm increases the reference voltage based on a fixed step voltage when,

The algorithm increases the reference voltage based on a fixed step voltage when,

$$\frac{\mathrm{dIpv}}{\mathrm{dVpv}} > 0 >0 \tag{2.10}$$

While it decreases the reference voltage using the fixed step voltage when

$$\frac{\mathrm{dIpv}}{\mathrm{dVpv}} < 0 \tag{2.11}$$

The INC algorithm offers several advantages over the P&O method, particularly in terms of its ability to more accurately track the MPP under rapidly changing environmental conditions. Because INC directly calculates the slope of the P-V curve, it can adjust the operating voltage more precisely, reducing the oscillations around the MPP and improving the overall efficiency of the system. However, INC is more complex to implement and requires higher computational resources, making it more suitable for larger PV systems where the performance benefits justify the added complexity. Here is the flow chart for INC algorithm.

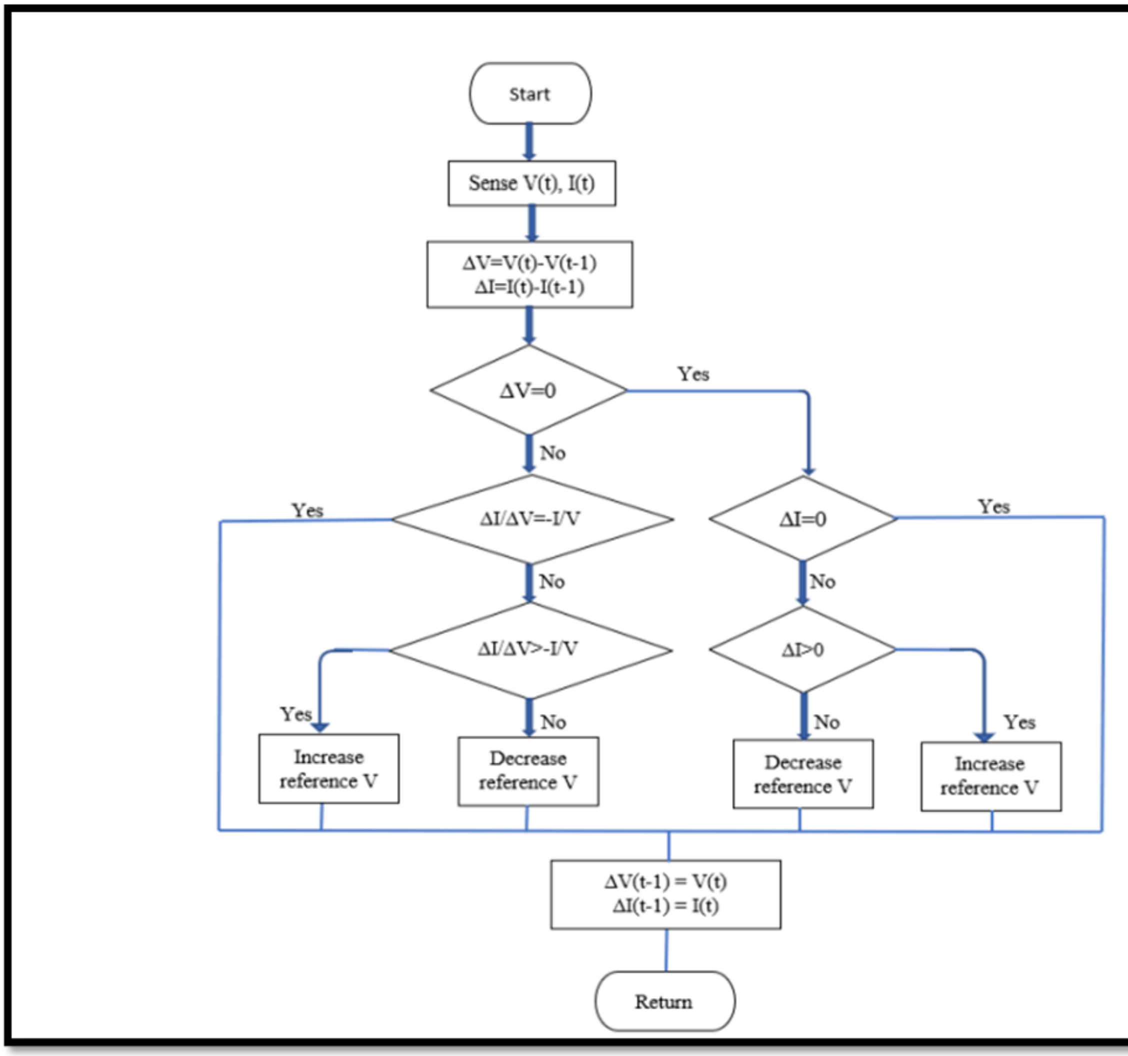

Figure 2.2 The flow chart for INC algorithm

2.3.1 Strengths

One of the key advantages of the INC algorithm is its ability to track the MPP more accurately than P&O, particularly under rapidly changing environmental conditions. By directly calculating the slope of the P-V curve, the algorithm reduces oscillations around the MPP and improves the overall tracking accuracy. This makes INC a suitable choice for applications where precision and performance are critical, such as in large-scale PV systems and systems operating in regions with frequent shading or rapidly changing weather conditions.

2.3.2 Weaknesses

Despite its improved tracking accuracy, the INC algorithm is more complex to implement than P&O. It requires more computational resources and hardware capability, making it less suitable for small-scale or low-cost PV systems. Additionally, INC's increased complexity can result in longer tracking times in some scenarios, which may reduce the algorithm’s overall speed in comparison to simpler techniques.

2.4 Particle Swarm Optimization (PSO)

In recent years, the application of metaheuristic algorithms, such as Particle Swarm Optimization (PSO) and Genetic Algorithm (GA), has gained traction in the field of MPPT for solar PV systems[61]. These algorithms are inspired by natural processes and employ a population-based search strategy to find the global maximum in a search space, making them well-suited for tracking the MPP in complex and dynamic environments, such as systems affected by partial shading[62].

Particle Swarm Optimization (PSO) is a bio-inspired algorithm based on the social behavior of birds flocking or fish schooling. In the context of MPPT, PSO operates by initializing a population of candidate solutions (particles) that explore the P-V curve in search of the MPP[63]. Each particle adjusts its position in the search space based on its own experience and the experience of neighboring particles. The algorithm iteratively updates the position of each particle, moving towards the point of maximum power with each iteration. PSO has been shown to offer fast convergence and high accuracy in tracking the MPP, especially in scenarios involving partial shading where multiple local maxima may exist[64]. By utilizing a global search strategy, PSO is able to avoid getting trapped in local maxima, a common problem faced by traditional MPPT algorithms like P&O and INC[65]. The PSO algorithm is as follows:

The position vector is given by equation

$$X = [X1, X2, \ldots, Xn] \tag{2.12}$$

The Velocity vector is given in Equation (2.12)

$$V = [V1, V2, \ldots, Vn] \tag{2.13}$$

Particle's best position and Global best position are given in Equations (16) and (17) respectively

$$Pbest = [Pbest1, Pbest2, \ldots, Pbestn] \tag{2.14}$$

$Gbest = [Gbest1, Gbest2, \ldots, Gbestn]$ (2.13)

The update equation is given in Equation (2.14).

$$Vnew = w * V + c1 * rad() * (Pbest - X) + c2 * rand() * (Gbest - X) \tag{2.15}$$

The position update as

$$Xnew = X + Vnew \tag{2.16}$$

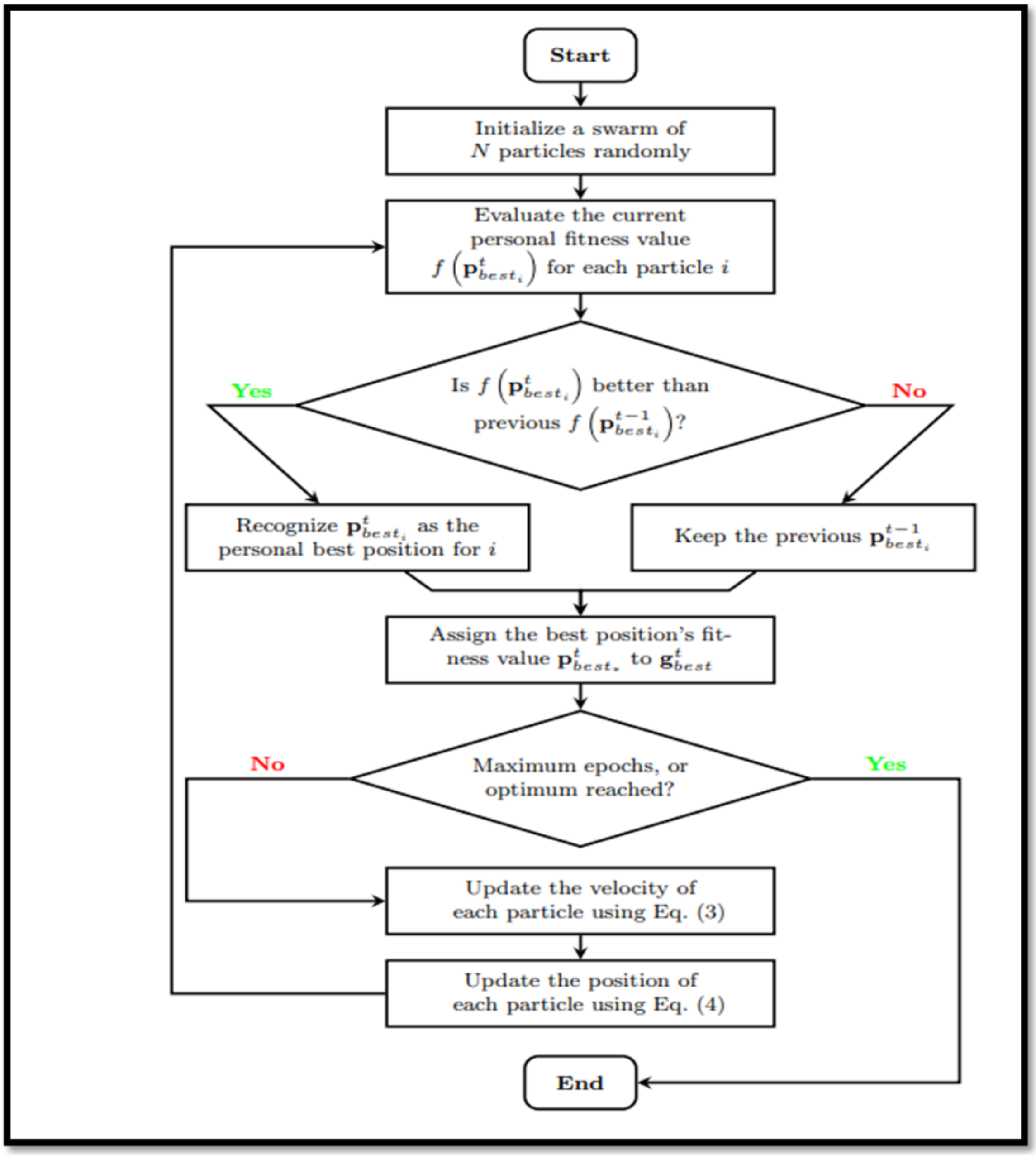

Figure 2.3 The flow chart for PSO algorithm[66]

2.4.1 Strengths:

PSO offers several advantages over traditional MPPT techniques like P&O and INC. First, it is highly effective in environments with multiple local maxima, such as solar PV systems affected by partial shading[67]. Unlike traditional algorithms, which may become trapped in local maxima, PSO employs a global search strategy that allows it to explore the entire search space and converge towards the global MPP. Additionally, PSO exhibits fast convergence rates, making it well-suited for large-scale and complex PV systems where tracking speed and accuracy are crucial.

2.4.2 Weaknesses:

The main drawback of PSO is its increased computational complexity[68]. The algorithm requires sophisticated hardware and higher processing power to manage the population of particles and perform the necessary calculations. As a result, PSO may not be suitable for small-scale or low-cost PV systems where simplicity and cost-effectiveness are prioritized[69]. Moreover, the effectiveness of PSO depends on the proper tuning of parameters, such as particle velocity and position updates, which can complicate the implementation process.

2.5 Genetic Algorithm (GA)

Genetic Algorithm (GA) is another metaheuristic technique that has been applied to MPPT in PV systems[70]. GA is based on the principles of natural selection and evolution, where a population of candidate solutions (individuals) evolves over time through processes such as selection, crossover, and mutation[71]. In MPPT applications, GA begins by generating an initial population of potential solutions. Each solution is evaluated based on a fitness function, which in this case would be the power output of the

PV system[72]. The best-performing solutions are then selected to create a new generation, which undergoes crossover and mutation to explore new regions of the search space[73]. Over successive generations, the algorithm converges towards the global MPP. GA, like PSO, is particularly effective in complex environments with multiple local maxima, as it can explore the entire search space to find the optimal solution.

To analyze the performance of the GA-based MPPT algorithm, it adjusts the algorithm parameters (population Size, and mutation Rate) and observes the best solution and fitness value obtained after the iterations. The initial parent population, denoted as array A, is initialized to start the optimization process. It consists of individual parent solutions represented by Xi = [parent 1, parent 2, . . ., parent n], where n represents the population size. Each parent solution, parent i where (i = 1, 2, . . ., n), corresponds to the initial voltage values at the beginning of the algorithm. The objective function, f(Xi), is used to calculate the output power of the PV system. The fitness values for each position in the population are evaluated based on this objective function[74]. These fitness values are essential for evolving the population and improving the overall fitness of the individuals over successive generations. The GA-MPPT conditions for the PV voltage and power are given as:

$$|V(k+1) - V(k)| < dV \tag{2.17}$$

$$|P(k+1) - P(k)| < dP \tag{2.18}$$

2.5.1 Strengths:

Like PSO, GA is highly effective in environments with multiple local maxima, making it suitable for PV systems affected by partial shading. GA's global search strategy allows it to explore a wide range of operating points, reducing the likelihood of becoming trapped in local maxima[75]. Additionally, GA is flexible and can be adapted to different system configurations and optimization criteria, making it a versatile solution for complex PV applications.

2.5.2 Weaknesses:

The primary disadvantage of GA is its computational complexity and the need for real-time processing capability[76]. Like PSO, GA requires sophisticated hardware to manage the population of solutions and perform genetic operations, which may limit its applicability in smaller, low-cost PV systems. Furthermore, the convergence speed of GA can be slower than that of PSO, particularly in large search spaces, which may impact the overall tracking performance under rapidly changing conditions.

CHAPTER THREE

OVERVIEW OF SWITCHED CAPACITOR CONVERTER TOPOLOGIES

Switched capacitor converters have gained popularity in the field of renewable energy, particularly in solar photovoltaic (PV) systems, due to their ability to achieve high voltage gains without inductors. In this chapter, various switched capacitor topologies are discussed, each offering unique benefits and applications in power electronics.

3.1 DC – DC Converter

The use of DC-DC converters is indispensable in a wide variety of applications, including residential, commercial, and industrial ones. A crucial function of these devices is to convert voltage, allowing seamless integration of devices operating at different voltage levels [77]. Through the efficient stepping up or stepping down of voltages, DC-DC converters contribute to the improvement of power supply efficiency and the reduction of energy losses during transmission and distribution. As essential components of renewable energy systems, they facilitate the storage and conversion of energy from solar and wind sources[29]. During the operation of electric vehicles, DC-DC converters contribute to the efficient transfer of energy from the battery pack to various components, thereby improving the overall performance[78]. During industrial applications, they help ensure power supply stability, support automation and data centers, and contribute to power quality and reliability. Further, DC-DC converters make it possible for electronic devices to be made smaller and more portable while maintaining reliable power supplies[79]. Modern electrical systems require versatility and efficiency to operate effectively, which makes them indispensable for the advancement of technology and efficient utilization of energy.

3.2 Switched Capacitor Converter

The switched capacitor converter (SC) is a particular type of direct current to direct current (DC-DC) converter that is based on combining capacitors and switches to conserve charge[80]. This device operates fundamentally in a cyclical manner, and it draws its power from the input voltage to charge the capacitor and then discharges that capacitor to the output under the influence of an output voltage. The first stage of the cycle is the conversion from one direct current level to another, which allows for a seamless power transfer between the source and destination of the power [81],[8]. In the context of inductive converters, SC converters are distinguished from inductive converters because they do not require inductors to operate[82].

3.3 Switched-Capacitor Topologies

An analysis of the topology of switched-capacitor converters provides a deeper insight into the complex construction and how these devices are constructed. Normally, it refers to the specific configuration of a SC converter that consists of capacitors, switches, and their connections, which can be adjusted and modified according to the output requirements and efficiency requirements of the converter. In the industry, the most prevalent topologies that are commonly used are the series, parallel, ladder and Fibonacci configurations that are used most [83].

3.3.1 Fibonacci Topology

The Fibonacci topology utilizes a combination of switches and capacitors that are unique in the fields of power electronics and makes it a unique solution[83],[84], [85]. Although they are characterized by an extremely unique design, they can be used to convert voltages between step-up and step-down, making them adaptable to various power supply requirements. In addition to their precision voltage levels, they help meet a wide range of power supply requirements with their flexible design and operation, resulting in flexible and effective solutions.

The Fibonacci SC converter arranges capacitors in a Fibonacci sequence (1, 1, 2, 3, 5, 8, etc.) to progressively step-up voltage levels. This topology provides a more gradual and efficient voltage boost compared to traditional converters. [8]demonstrated that when integrated with advanced MPPT algorithms, the Fibonacci SC converter offers improved performance in voltage regulation, making it ideal for solar PV systems.

The k-Fibonacci designs, on the other hand, presents some limitations despite its advantages, even though it uses switched capacitor technology. The design and operation of the k-Fibonacci SC DC-DC converter may pose challenges in terms of manufacturing, maintenance, and error detection since the converter is inherently complex. Additionally, the practical applicability of this technology could be constrained by specific application requirements and the need for rigorous real-world testing and validation to mitigate the risk of additional costs and time expenditures[86].

3.3.2 Doubler Topology

The doubler topology is designed to double the input voltage by charging capacitors in parallel and discharging them in series. This topology is efficient in low-power applications and offers relatively simple control, but its voltage gain is limited, making it less suitable for large-scale solar PV systems.

This circuit is powered by a source of AC alternation and operates in two stages, depending on how the power is applied to it. The first one creates a voltage peak in the capacitor that matches the peak value of the source voltage. Second, the previously charged capacitor is connected in series with the load by placing a load in parallel with the source of power, which then supplies power to the load. The series of voltages that are generated by this combination are ideally the same as twice the voltage that is input into the system[87], [88].

3.3.3 Series-Parallel Topology

There is a flexibility of this converter that comes from the fact that every cell can be arranged in series or parallel, and the output voltage can be modified at any time, hence allowing the converter to be used in different applications. During the energy transfer from the input to the output the capacitors are connected in parallel with the source, resulting in energy transfer from the input to the output.

Once the capacitors have successfully been arranged in series, in a short amount of time the load will be supplied by the capacitors. It is important to point out that this arrangement for this converter has some remarkable advantages over the Cockcroft Walton Voltage Multiplier, there are some noticeable advantages to this arrangement, particularly in terms of the high output impedance, because it does not have the same problems as the Cockcroft Walton Voltage Multiplier. Despite this, there are a few drawbacks to this method, such as the fact that many capacitors are being charged at the same time, which could require a large amount of current from the source over a short period of time. Additionally, if many capacitors are being charged at the same time, the voltage ripple at the output may also be high, thereby affecting the efficiency of the converter directly. There is still the possibility that parasitic capacitances may cause problems with your circuits when you increase the voltage, depending on how long the connection tracks are on the printed circuit boards (PCBs) and how the elements are arranged, as well as how many capacitors there are. In the event of high voltage gains, parasitic capacitances significantly reduce the efficiency of the circuit[89].

3.3.4 Ladder Topology

This ladder cell configuration can be arranged in a boost and buck configuration to achieve the desired output voltage[90]. This type of converter can be built with one or more cells depending on how high the conversion ratio should be according to the topology of the converter. Ladder topology converter traditionally works in a voltage step-up mode, in which the source is connected in series with n capacitors that are charged with a voltage called Vi[91]. Flying capacitors can be connected to a source of electricity at a given time in parallel with the source of electricity that is to be charged. However, after that, it will be connected in parallel with another capacitor so that it can also be charged by Vi later. This is done to obtain a voltage Vo because of connecting the voltage source in series with the n charged capacitors and following Equation 23.

$$V_o = V_i + nV_i \tag{3.1}$$

This converter operates in a similar manner to a capacitive voltage divider if used as a step-down topology, in which the load is connected in parallel with one of the capacitors and the converter has been constructed as a series of n capacitors in series. A capacitor that is connected in parallel to the source is also included in this circuit, as well as one or more flying capacitors that may be associated in parallel with the elements making up the capacitive divider at any given time. Because of this arrangement, the output voltage of the converter will vary depending on the number of capacitors that are used in the converter, as defined by Equation 25.

$$Vo = \frac{\mathrm{Vi}}{\mathrm{ncap}} \tag{3.2}$$

The number ncap indicates the number of series capacitors included in the converter. A topology of this type can also be used in AC-AC conversion, with good regulation as well as a high-power factor, making it a viable alternative to ferromagnetic core transformers for AC-AC conversion[42].

3.3.5 Dickson Charge Pump

According to Dickson, a charge pump will only operate in a steady state when its output voltage is limited to a constant value when its output voltage is constant. At steady state conditions, the charge transferred from one capacitor to the next equals the charge transmitted from the input to the output. The charge pump will remain in a steady state while running even during the boost process if the rise time of the output voltage is sufficiently long compared with the clock cycle time of the clocks driving the charge pump, which is to say the output voltage rises slowly. It is necessary to consider the load capacitance of the charge pump itself in order to take the total charge consumed by the charge pump into account[92].

3.4 Conventional Boost Converter

A boost converter is a type of DC-DC converter which serves as a step-up converter in that it can convert input voltages into higher output voltages when used effectively. DC-DC converter operates on two key phases as part of its operation mechanism. The ON phase and the OFF phase can be considered as the key phases of how the converter operates. In the "ON" phase of the circuit, energy is stored in the inductor while the transistor is turned on, while in the "OFF" phase, the energy is redirected to the load after the stored energy in the inductor is released. With the aim of maintaining control over the output voltage, the duty cycle is responsible for regulating the ratio of times that the output voltage will be on and off. There has been extensive application of Boost Converters owing to these characteristics that include electric vehicles, renewable energy systems, and correction of power factors in electric drives. A capacitor is used to store energy in an inductor, which is then delivered to the load through an inductor, to deliver it to the load[93], [94], [95], [96].

Several recent advancements and trends in boosting converter technology have been geared towards improving the efficiency of the devices, downsizing the devices, and addressing electromagnetic interference (EMI) issues that may arise. In terms of advancements, these can be categorized broadly as the introduction of advanced control strategies and the incorporation of GaN (Gallium Nitride) devices into the design of the boost converter, which contribute to the significant improvement of efficiency and the reduction in size [97].

3.5 Fibonacci Sequence Design and Modeling

3.5.1: Convectional Fibonacci Switched capacitor

The Fibonacci sequence-based SC converter offers a novel approach to voltage boosting by arranging capacitors in a Fibonacci series. This design increases voltage gains incrementally, resulting in better efficiency and stability. Authors in [8] developed a detailed MATLAB/Simulink model of this converter, demonstrating its superior performance in handling dynamic load changes and providing stable voltage output in solar PV applications.

Fibonacci Sequence Switched Capacitor converter (FSSC). Figure 3.1 displays the schematic diagram of a Fibonacci sequence SC converter. It entails 10 switches (transistor, 3 capacitors, and output capacitors). Switches are used to turn ON and turn OFF the converter that functions in several switching states with suitable gains[42].

The converter was operated by using the rule of Table 1. The odd number switches are operational in stage 1, and the even number switches are operational in stage 2. In this converter the voltage gain is increased gradually in each stage based on Fibonacci sequence number (1, 2, 3, 5, 8, 13, 21, …), the value of voltage in the capacitor becomes V_{in}, $2V_{in}$, $3V_{in}$ and $5V_{in}$.

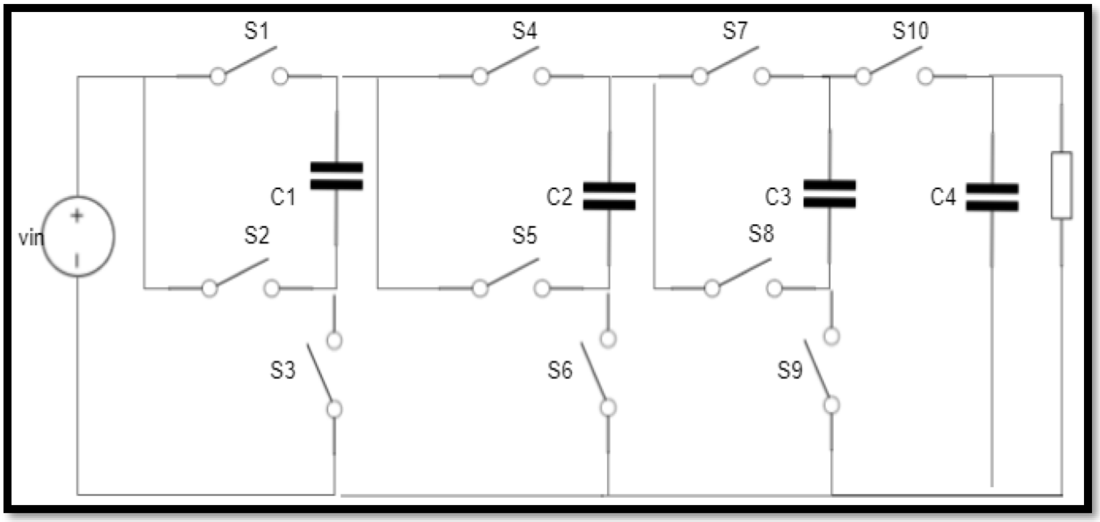

Figure 3.1 Schematic diagram of 3rd stage Fibonacci sequence SCBC.

Step	Switches to Turn ON	Switches to Turn OFF
Mode 1	S1, S3, S5, S7, S9	S2, S4, S6, S8, S10
Mode 2	S2, S4, S6, S8, S10	S1, S3, S5, S7, S9

Table 3.1 Switching rule of conventional Fibonacci sequence SC converter.

The output voltage is [1]

$$Vout = Vin + Vin \times \sum_{n=1}^{k} F_n \quad (3.3)$$

Where F_n is the Fibonacci sequence number F_1= 1, F_2= 1, for n ≥ 3, F_n= F_{n-1}+ F_{n-2}

K: the stage's number.

Figure 3.2 shows the Fibonacci sequence converter stage 1. In this stage the converter operates 5 transistor switches that charge the C3 up to 3 times the input voltage. Figure 3 shows the Fibonacci sequence converter stage 2. In this stage, the converter operates 5 transistor switches that charge the C3 up to 5 times the input voltage and discharge the capacitor's energy into the output. By applying Kirchhoff's voltage and current laws (KCL, KVL) in each loop for mode 1 and 2 for Figure 2 and Figure 3, the state is calculated as follows:

The stage 1 on Figure 3.2

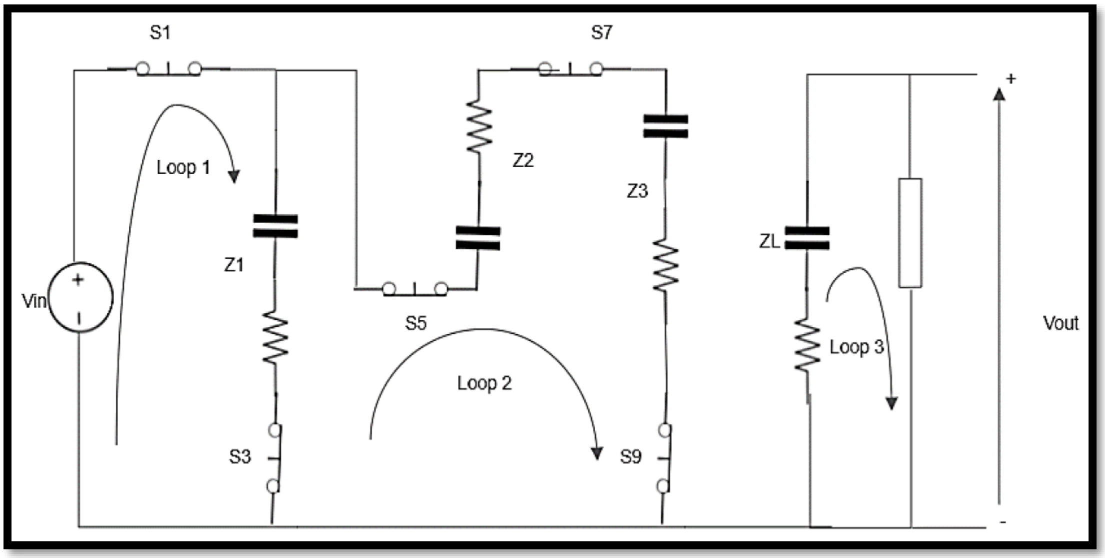

Figure 3.2 Mode 1 of Fibonacci SCBC.

Loop 1:

$$V_{in} = Z1\,(I1 - I2) \quad (3.4)$$

Loop 2:

$$0 = Z1 \times (I2 - I1) + Z2 \times I2 + Z3 \times I3 \quad (3.5)$$

Loop 3:

$$V_{out} = I3 \times ZL \quad (3.6)$$

The impedance Z1, Z2, and Z3 are the series combinations of R and C. The state space representation for Mode 1 is as follows.

$$\begin{bmatrix} V_{in} \\ 0 \\ V_{out} \end{bmatrix} = \begin{bmatrix} Z1 & -Z1 & 0 \\ -Z1 & Z1 + Z2 + Z3 & 0 \\ 0 & 0 & ZL \end{bmatrix} \begin{bmatrix} I1 \\ I2 \\ I3 \end{bmatrix} \quad (3.7)$$

The stage 2 on Figure 3.3

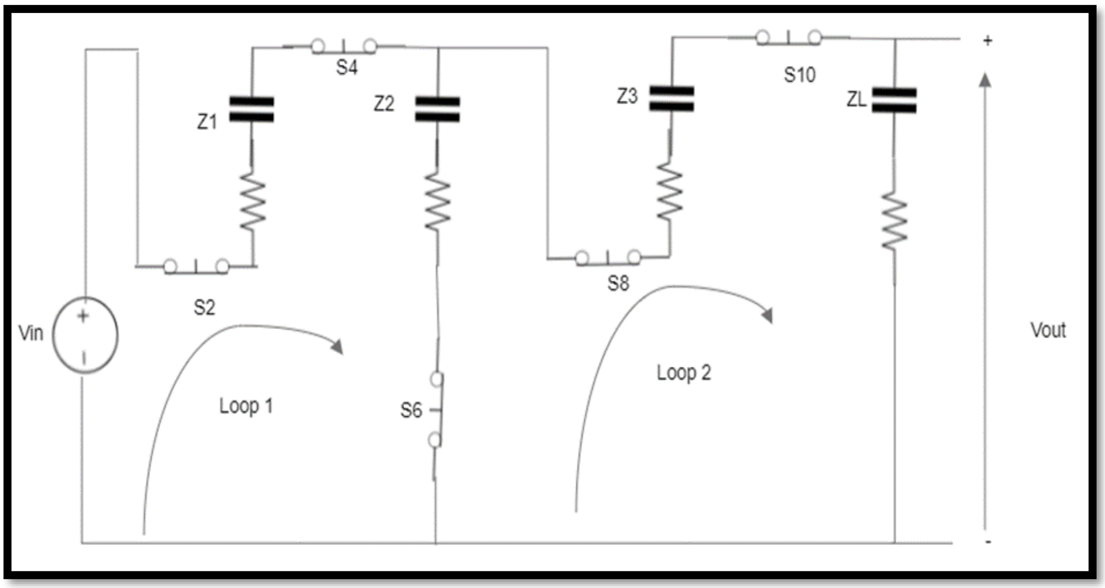

Figure 3.3 Mode 2 of Fibonacci SCBC

Loop 1:

$$V_{in} = I1 \times (Z1 + Z2) - I2 \times Z3 \quad (3.8)$$

Loop 2:

$$V_{out} = I3 \times ZL + (Z2 + Z3) \times I2 - Z2 \times I1 \quad (3.9)$$

The state space representation for Mode 2 is as follows:

$$\begin{bmatrix} V_{in} \\ V_{out} \end{bmatrix} = \begin{bmatrix} Z1 + Z2 & -Z2 & 0 \\ -Z2 & Z2 + Z3 & ZL \end{bmatrix} \begin{bmatrix} I1 \\ I2 \\ I3 \end{bmatrix} \quad (3.10)$$

3.5.2: Improved Fibonacci Switched Converter

Figure 3.4 illustrates a schematic diagram for the improved Fibonacci switched capacitor converter. It contains six Metal Oxide Semiconductor Field Effect (MOSFET) transistors, three capacitors, four diodes, and output capacitors. MOSFETs are used to turn on and off the converter that functions in several switching states with appropriate gains[98]. In stage 1, the MOSFETs with odd numbers are operational, while in stage 2, the MOSFETs with even numbers are operational. In this converter, the voltage gain increases gradually in each stage based on Fibonacci sequence numbers (1, 2, 3, 5, 8, 13, 21, ...), resulting in Vin, 2Vin, 3Vin, and 5Vin in the capacitor.

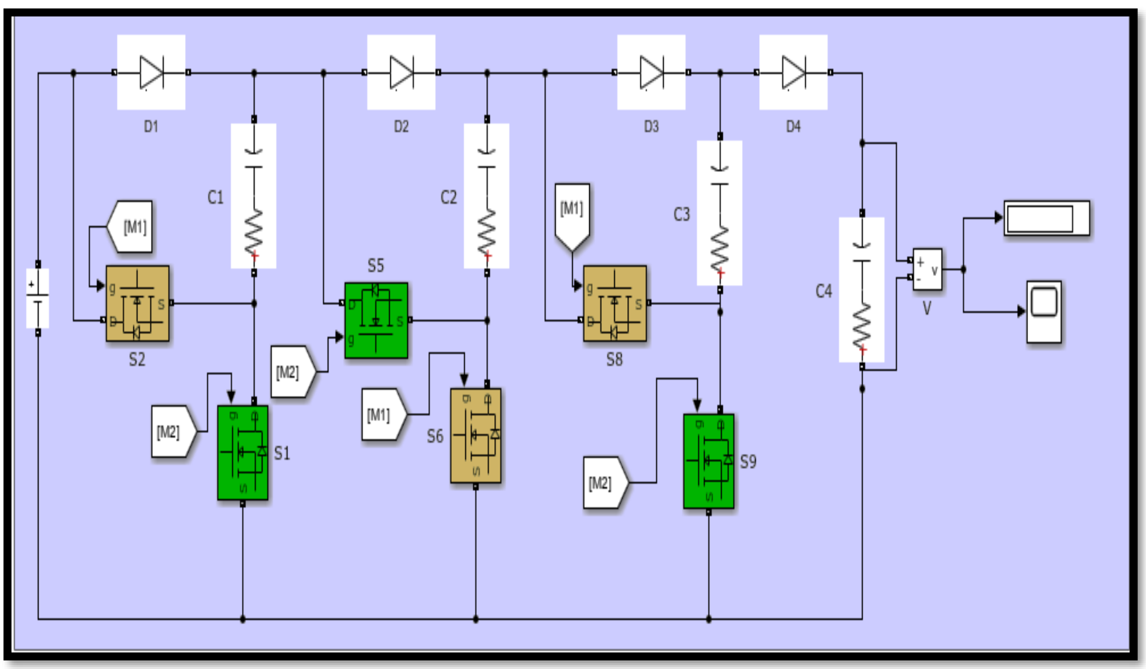

Figure 3.4 Improved Fibonacci Switched Capacitor Converter

The operational phases of circuit configuration above involved specific switches and diodes that dictate the current flow and energy transfer. The dynamic interaction of capacitors and the application of Kirchhoff's laws provide a foundation for analyzing the system's behavior. This setup ensures efficient energy management and transient response within the circuit.

In the first operational phase, switches S1, S5, and S9 are in the conducting state, while switches S2, S6, and S8 remain non-conducting. Diodes D1 through D4 are forward-biased, facilitating current flow through their respective paths[99]. Capacitors C1 to C4 interact dynamically, influencing the transient behavior of the circuit through charging and discharging processes. To analyze the circuit dynamics during this phase, Kirchhoff's Current Law (KCL) and Kirchhoff's Voltage Law (KVL) are applied to derive the governing equations for node voltages and loop currents. This framework ensures a systematic evaluation of energy transfer and steady-state transitions within the system.

Current in C_1:

$$Ic_1 = \frac{dvc_1}{dt} \tag{3.11}$$

Current C_2:

$$Ic_2 = \frac{dvc_2}{dt} \tag{3.12}$$

Current C_3:

$$Ic_3 = \frac{dvc_3}{dt} \tag{3.13}$$

Current C_4:

$$Ic_4 = \frac{dvc_4}{dt} \tag{3.14}$$

For input voltage Vin charges C_1, C_2, $C_3$and partially contributes to

The circuit's governing equations

V_{in}=Vc_1 + Vc_2 (3.15)

Vc_2= Vc_3 + Vc_4 (3.16)

On the other hand, In Phase 2 of operation, switches S2, S6, and S8 are conducting, allowing current to flow through their respective paths, while switches S1, S5, and S9 are non-conducting, isolating their circuits. Diodes D1, D2, D3, and D4 are reverse biased, preventing current flow in the reverse direction. During this phase, capacitors C1 discharge their stored energy into capacitors C2 and C3, transferring charge and ensuring the energy conversion process continues. The equations governing Phase 2 are derived using Kirchhoff's Current Law (KCL) and Kirchhoff's Voltage Law (KVL), which are applied to describe the dynamic behavior of the system during this phase. Here are the equations that govern the second phase.

Vc_1 = Vc_2+ Vc_3 (3.17)

Vc_3= Vc_4 (3.18)

The average equations combined both phases using the duty cycle D

Voltage across C_1:

$$\frac{dVc_1}{dt} = \text{D} \times \left(\frac{V_{in} - Vc_1}{Req_1}\right) + (1 - \text{D}) \times \left(\frac{-Vc_1 + Vc_2}{Req_2}\right) \quad (3.19)$$

Voltage across C_2:

$$\frac{dVc_2}{dt} = \text{D} \times \left(\frac{Vc_1 - Vc_2}{Req_3}\right) + (1 - \text{D}) \times \left(\frac{-Vc_2 + Vc_3}{Req_4}\right) \quad (3.20)$$

Voltage across C_3:

$$\frac{dVc_3}{dt} = \text{D} \times \left(\frac{Vc_2 - Vc_3}{Req_5}\right) + (1 - \text{D}) \times \left(\frac{-Vc_3 + Vc_4}{Req_6}\right) \quad (3.21)$$

Voltage across C_4:

$$\frac{dVc_4}{dt} = \mathrm{D} \times \left(\frac{Vc_3 - Vc_4}{Req_7}\right) \tag{3.22}$$

Figure 3.5 illustrates the pulse waveforms for M1 and M2, which govern the switching of the MOSFETs during the two-phase operation of the Fibonacci switched-capacitor converter. The top waveform, M1, drives the MOSFETs responsible for Phase 1, while the bottom waveform, M2, controls the MOSFETs for Phase 2. These pulses are generated by a PID controller and are precisely synchronized to ensure seamless alternation between the two phases. The pulses maintain a consistent frequency, with each phase being activated in a complementary manner, which is essential for efficient charge transfer and voltage regulation within the converter.

The synchronization of these pulses is critical for the converter's performance, as it ensures that energy is transferred smoothly between phases, minimizing energy losses and maintaining system stability. The precise timing and complementary nature of the pulses allow the converter to achieve the desired step-up voltage efficiently. This well-coordinated operation highlights the importance of the control mechanism in optimizing the converter's functionality and reliability.

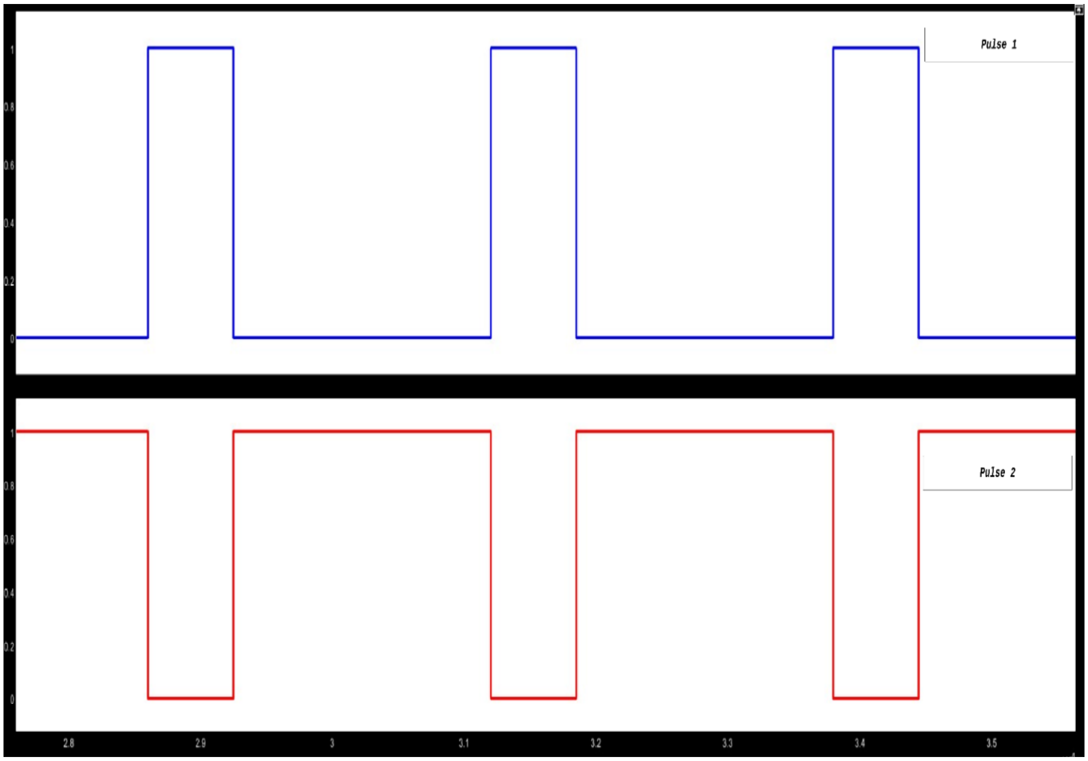

Figure 3.5 Pulse Waveforms for Phase 1 and Phase 2 Switching (M1 and M2)

Description	Value
Input Voltage	5V
Output Voltage	20V
Switching Frequency	80 KHz
Capacitance Values	22 µF
Resistance Values	30 mΩ

Table 3.2: Specification for simulation in MATLAB/Simulink

The PID controller plays a crucial role in optimizing the performance of the Fibonacci switched-capacitor converter by dynamically adjusting the width and timing of the M1 and M2 pulses based on real-time feedback from the output voltage. The Proportional (P) term fine-tunes the pulse timing to align with the desired voltage, ensuring quick response to changes. The Integral (I) term corrects accumulated errors over time, enhancing steady-state accuracy and minimizing long-term deviations. The Derivative (D) term predicts and mitigates future errors, reducing oscillations and improving overall system stability.

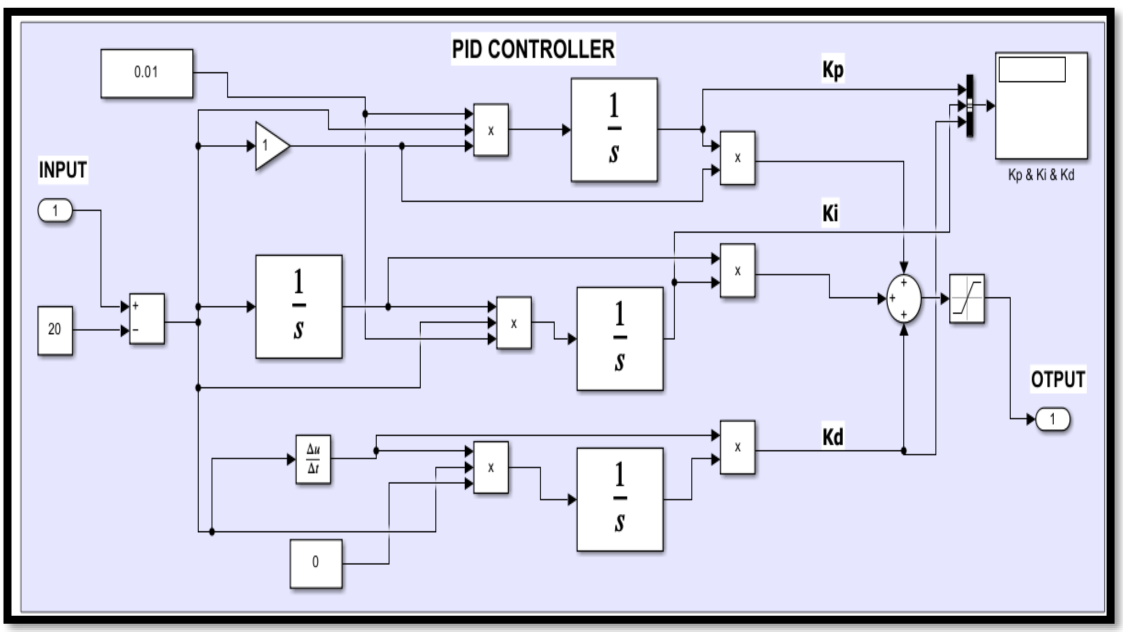

Figure 3.6 PID Controller Configuration

This sophisticated control mechanism ensures that the M1 and M2 pulses are precisely synchronized, facilitating smooth transitions between Phase 1 and Phase 2. Such synchronization is vital for efficient energy conversion, as it minimizes energy losses and maintains consistent voltage regulation. The real-time adjustments made by the PID controller enable the converter to adapt to varying load conditions and input fluctuations, ensuring robust and reliable operation. Figure 3.7 show the pulse control configuration.

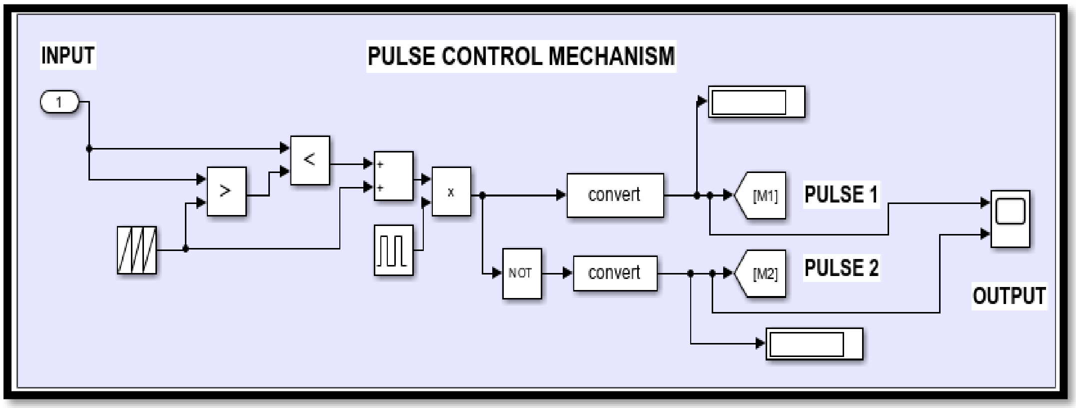

Figure 3.7 Pulse control mechanism

3.5.3: Hardware Implementation of Improved FSC

Figure 3.8 depicts the experimental setup designed to validate the performance of the proposed improved Fibonacci switched-capacitor converter. The setup includes essential components such as the converter circuit, measurement instruments, and control systems. This configuration allows for precise testing and analysis of the converter's efficiency, voltage regulation, and overall functionality under various operating conditions. The image provides a visual representation of the practical implementation, highlighting the integration of hardware and control mechanisms used to ensure accurate and reliable experimental results.

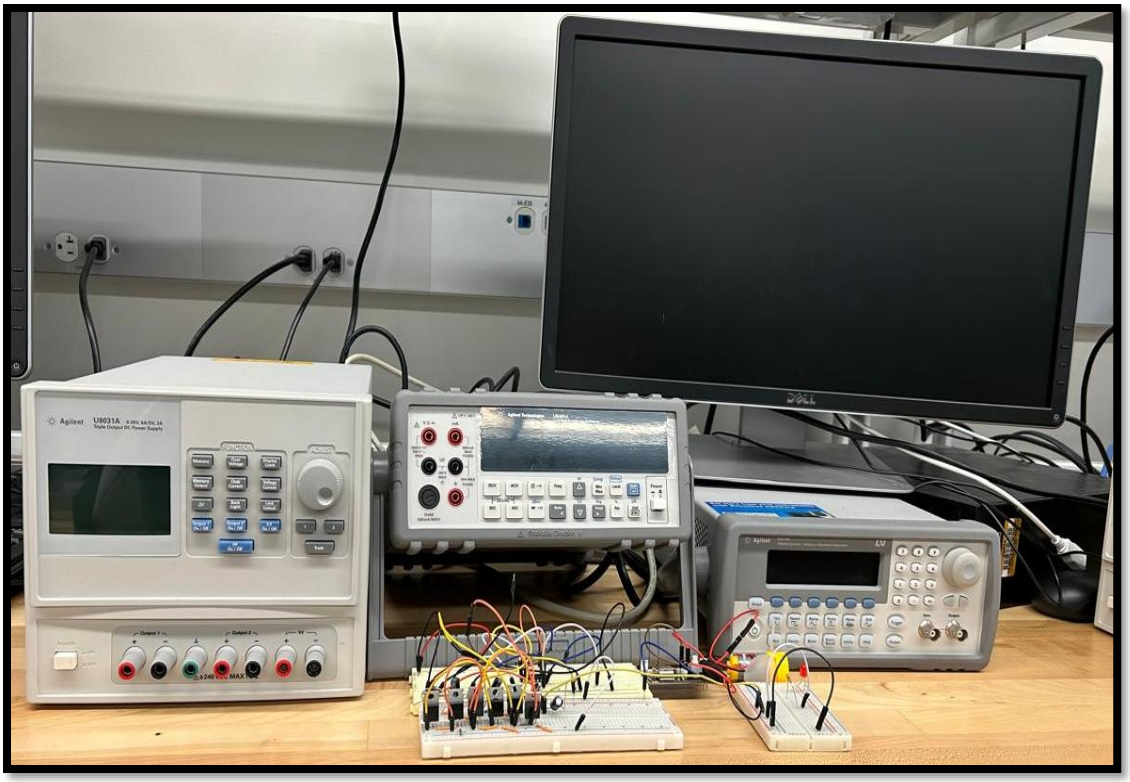

Figure 3.8 Setup for experimental

The abstract diagram in Figure 3.9 outlines the hardware implementation of the Fibonacci switched-capacitor converter system. The setup includes a DC power supply that provides the initial input voltage to the converter. The Fibonacci switched-capacitor converter, controlled by gate signals M1 and M2, performs the voltage conversion. A voltage regulator ensures stable output, while a function generator controls the switching signals. The system supports various load types, including a resistive load and a DC motor, allowing for comprehensive testing under different conditions. This configuration demonstrates the integration of key components to achieve efficient voltage conversion and regulation in practical applications.

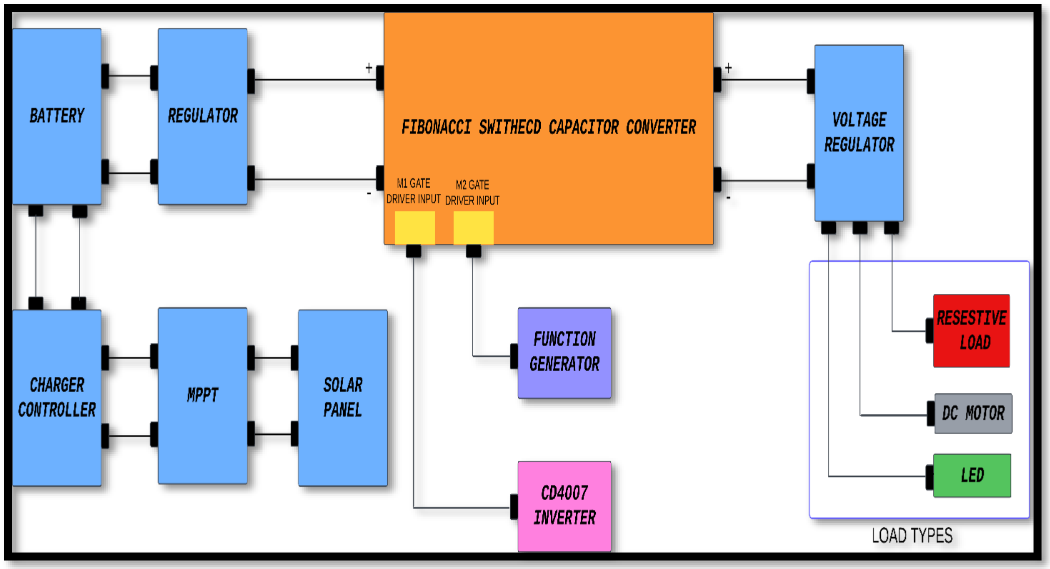

Figure 3.9 System Abstract Diagram for Hardware Implementation

The CD4007 IC is utilized as a gate driver to control the switching operation of the MOSFETs in the Fibonacci switched-capacitor converter. It generates complementary gate drive pulses for Phase 1 switches (S1, S5, and S9) and Phase 2 switches (S2, S6, and S8). These complementary signals are essential for ensuring the synchronized alternation of phases, which facilitates efficient charge transfer and voltage regulation. A function generator provides a square wave signal that is processed by the CD4007 to produce the necessary control signals for the two phases. Specifically, Pin 6 of the CD4007 drives the gates of S1, S5, and S9, while Pin 8 drives the gates of S2, S6, and S8. This precise synchronization between the phases is crucial for enabling efficient charge transfer processes and maintaining the stability of the converter. Figure 3.10 illustrates the circuit configuration of the CMOS Dual Complementary Pair Plus Inverter, highlighting the connections and signal flow within the gate control system.

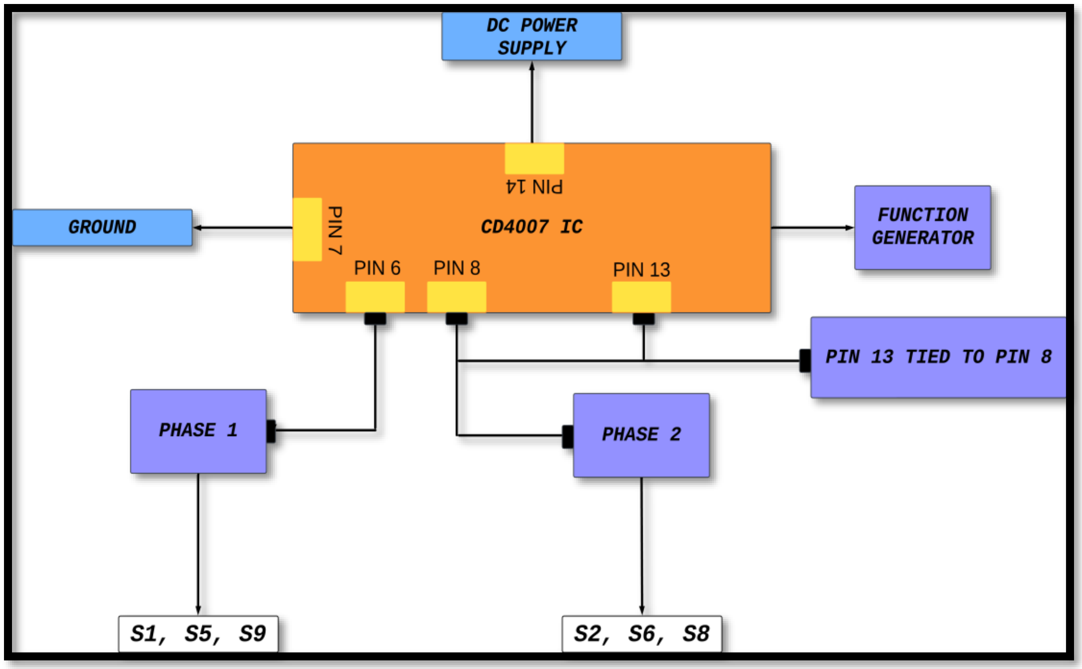

Figure 3.10 Configuration Circuit CD4007

Figure 3.11 illustrates the experimental hardware setup for the Fibonacci switched-capacitor converter, showcasing the physical implementation of the system. The setup includes critical components such as the CD4007 IC, which controls the switching MOSFETs, and the output regulation circuit, ensuring stable voltage output. The prototype was tested using a 5V DC motor and an LED light, both of which operated as expected, confirming the converter's ability to deliver consistent voltage and efficient power regulation under varying load conditions.

The CD4007 IC plays a pivotal role in generating complementary gate drive signals for the MOSFETs, enabling synchronized switching between Phase 1 and Phase 2. This synchronization is essential for efficient charge transfer and voltage regulation. The output regulation circuit further enhances the system's stability, ensuring that the voltage remains consistent even when the load changes. The successful operation of the DC motor and LED light demonstrates the converter's robustness and reliability in real-world applications.

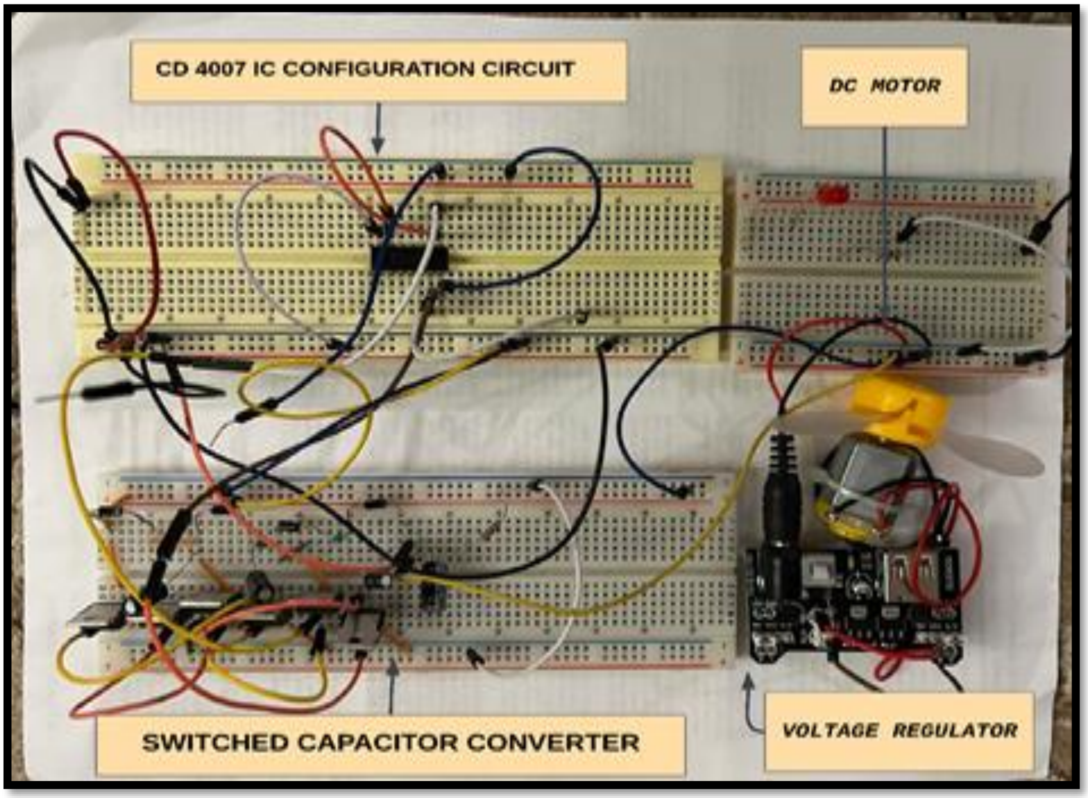

Figure 3.11 Breadboard Prototype of the FSC Converter Circuit

3.6 Boost Converter Design and Modeling

Boost converters are designed using specific configurations of capacitors, inductors, and switches. The design of the converter involves trade-offs between size, efficiency, and response time. MATLAB/Simulink is frequently used to simulate and model the performance of these converters under different operating conditions.

Fig. 3.12 displays the conventional boost converter. The output voltage is greater than the input voltage S1 was used as turn ON and turn OFF to achieve the desired output voltage. The function of boosting DC-DC converter can be split up into two states, Mode 1 and Mode 2. In mode 1, S1 turns ON, the input current rises linearly and flows through the inductor L1, S1 and diode D1 is on reverse bias acting as open switch. In mode 2, S2 turns OFF, the stored current in the inductor flows through the C1, resistive load and D1 is on forward bias acting as closed switch. Fig. 3.13 and Fig. 3.14 illustrate the two modes of circuit's operation.

The voltage and current relation for inductor L1 in figure 3.12 as follows

$$\frac{diL}{dt} = \frac{V_{in}}{L} \tag{3.23}$$

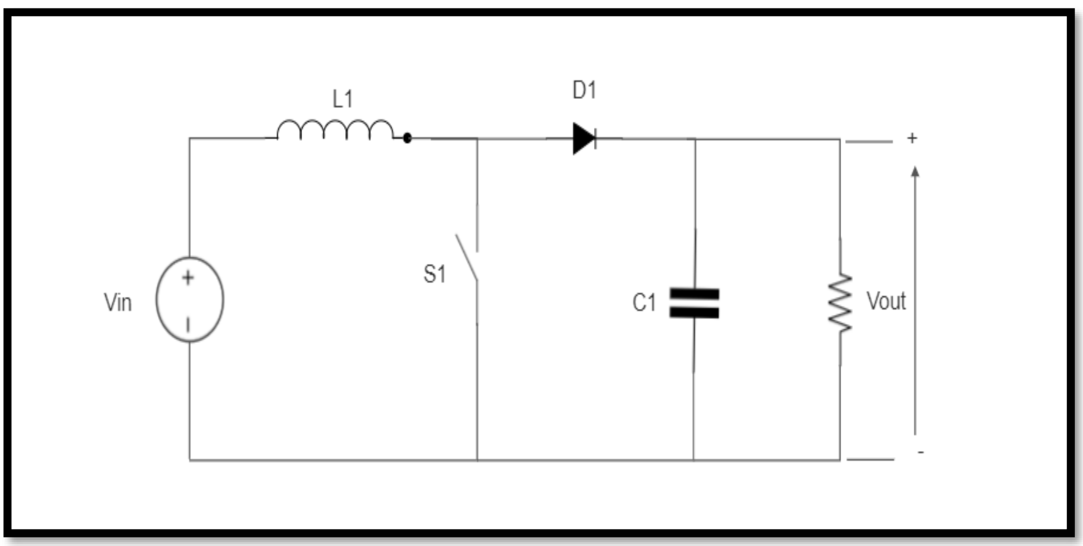

Figure 3.12 Boost converter

When the switch S1 turns ON, the configuration was created, as shown in figure 3.13

$$\frac{diL}{dt} = \frac{(V_{in}-V_{out})\times Ton}{L} \tag{3.24}$$

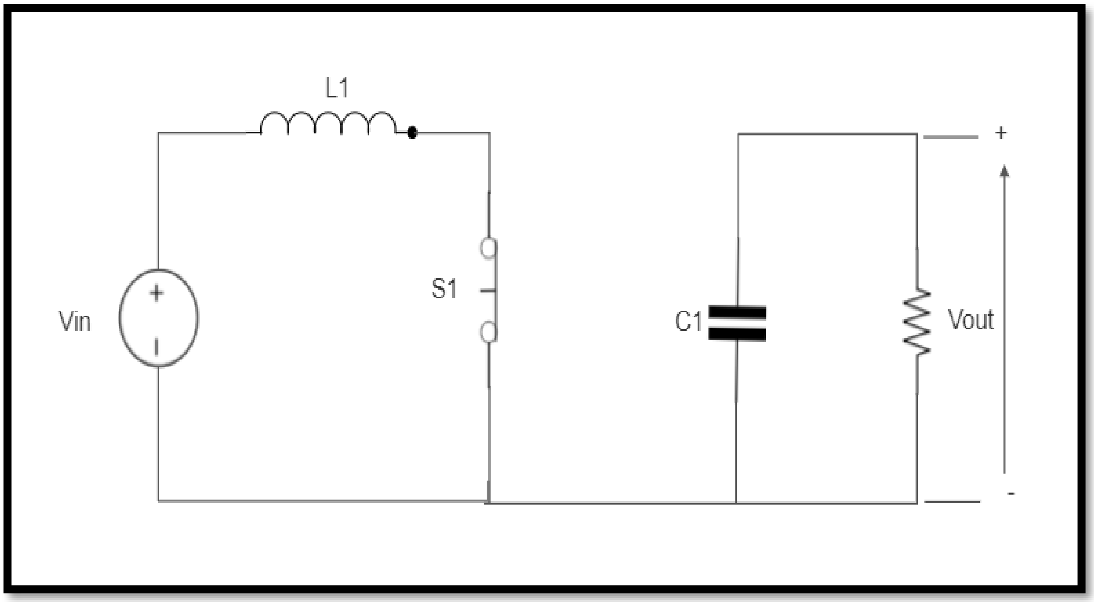

Figure 3.13 Boost converter Mode 1

When the switch S2 turns OFF, the configuration was created, as shown in figure 3.14

$$\frac{diL}{dt} = \frac{(V_{out} - V_{out} + Vd1) \times Toff}{L} \tag{3.25}$$

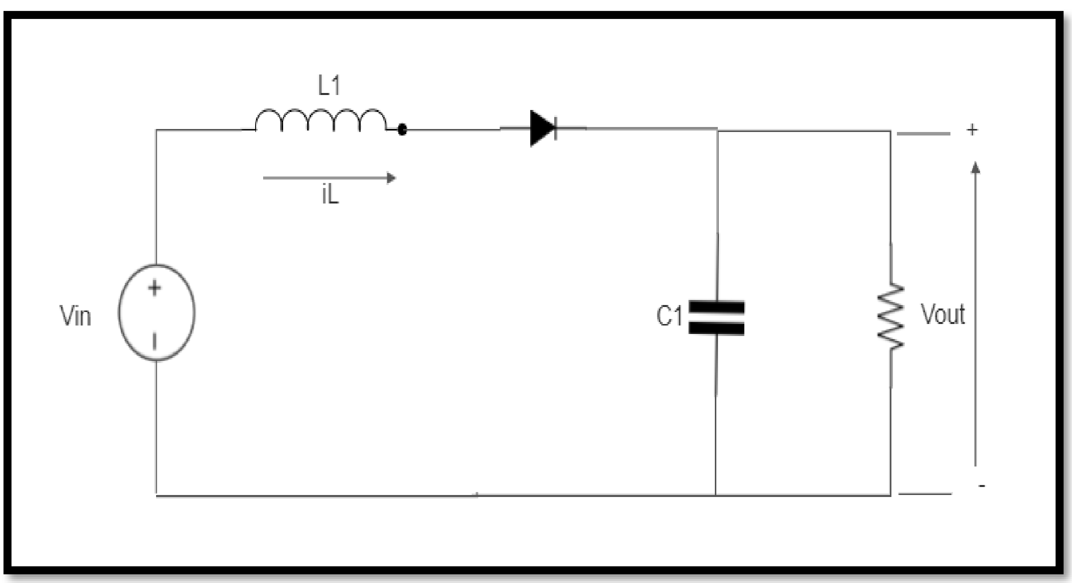

Figure 3.14 Operation of Boost converter Mode 2

The waveforms of voltage and current are shown on Figure 6. The selection between continuous conduction mode (CCM) and discontinuous conduction mode (DCM) depends upon factors including input voltage, output voltage, load current, and circuit parameters[100]. The interactions between the inductor's voltage and current waveforms and other converter components, such as the diode and output capacitor, play an important role in achieving both regulated output voltage and efficient energy transfer. The inductor within a conventional boost converter helps to accumulate and discharge energy to attain the desired output voltage. The inductor's current waveform undergoes phases of linear increase and decrease, while the inductor's voltage waveform is contingent upon the input voltage and characteristics of circuit components. The decision between continuous and discontinuous conduction modes substantially influences the behavior of inductor current throughout the switching cycle. waveforms of voltage output and current are shown on Fig. 3.15.

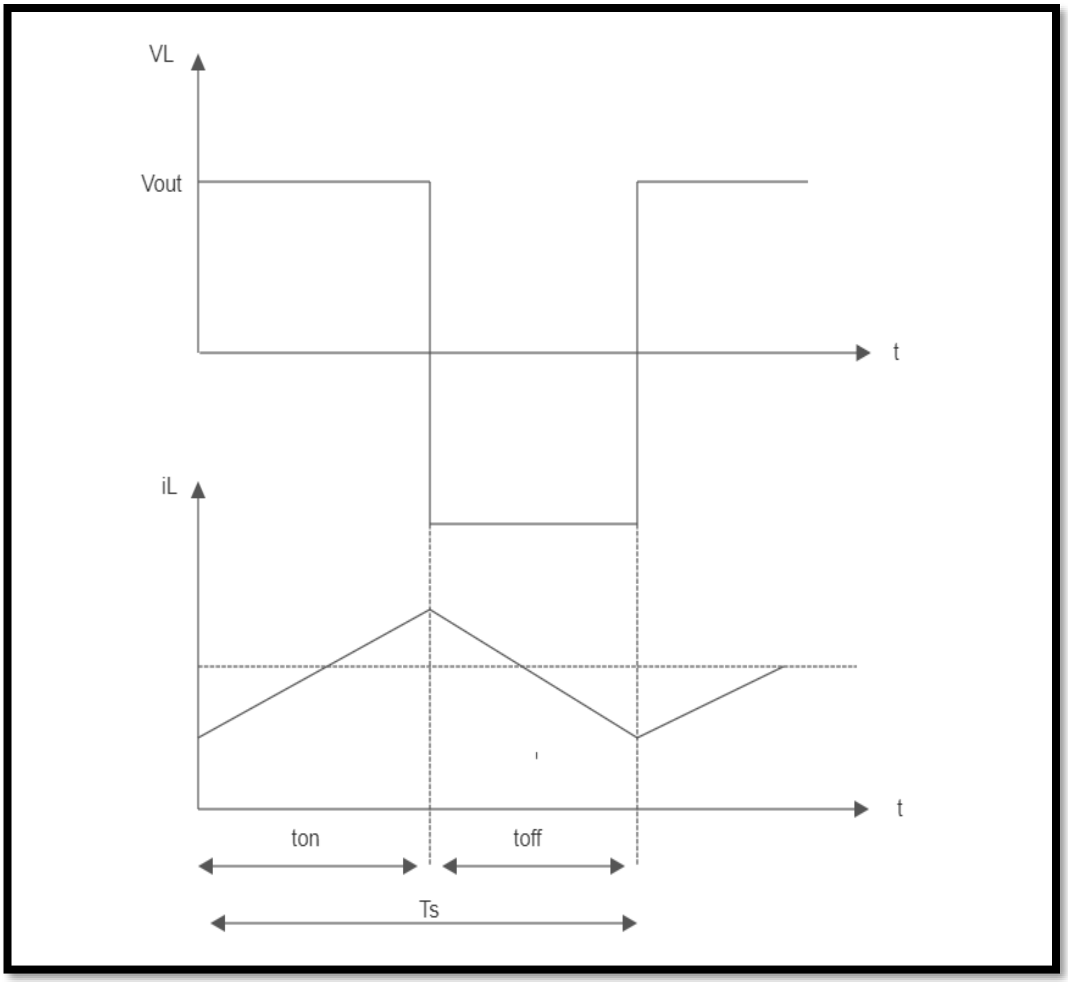

Figure 3.15 Waveform of output voltage and current

CHAPTER FOUR

COMPARATIVE PERFORMANCE EVALUATION OF BOOST AND FIBONACCI SWITCHED CAPACITOR CONVERTERS FOR SOLAR PV INTEGRATION

This chapter presents a detailed comparative evaluation of the conventional boost converter and Fibonacci switched capacitor converter, focusing on their performance in solar PV systems. The analysis is conducted through MATLAB/Simulink simulations, using dynamic MPPT algorithms to assess their efficiency, voltage regulation, and power handling capabilities.

The simulation figures depict the verification of the proposed switched capacitor configuration. Figure 4.1 shows the PV characteristics of the SunPower SPR-440NE-WHT-D, while Figure 8 shows the current vs. voltage and power vs. voltage characteristics for one module. The number of parallel strings (N_p) is seven and series connected modules per string (N_s) is six for the conventional boost converter (the total number of PV panels is 42). On the other hand, the number of parallel strings is three and series connected modules per string is three for the switched capacitor boost converter (the total number of PV panels is 9). The irradiance and temperature are maintained at a constant as 100 W/m^2 and 25 °C, respectively. The complete MATLAB/Simulink for the conventional boost converter and the proposed switched capacitor (Fibonacci) is shown in Figure 4.4

Figure 4.1 MATLAB/Toolbox PV panel specifications

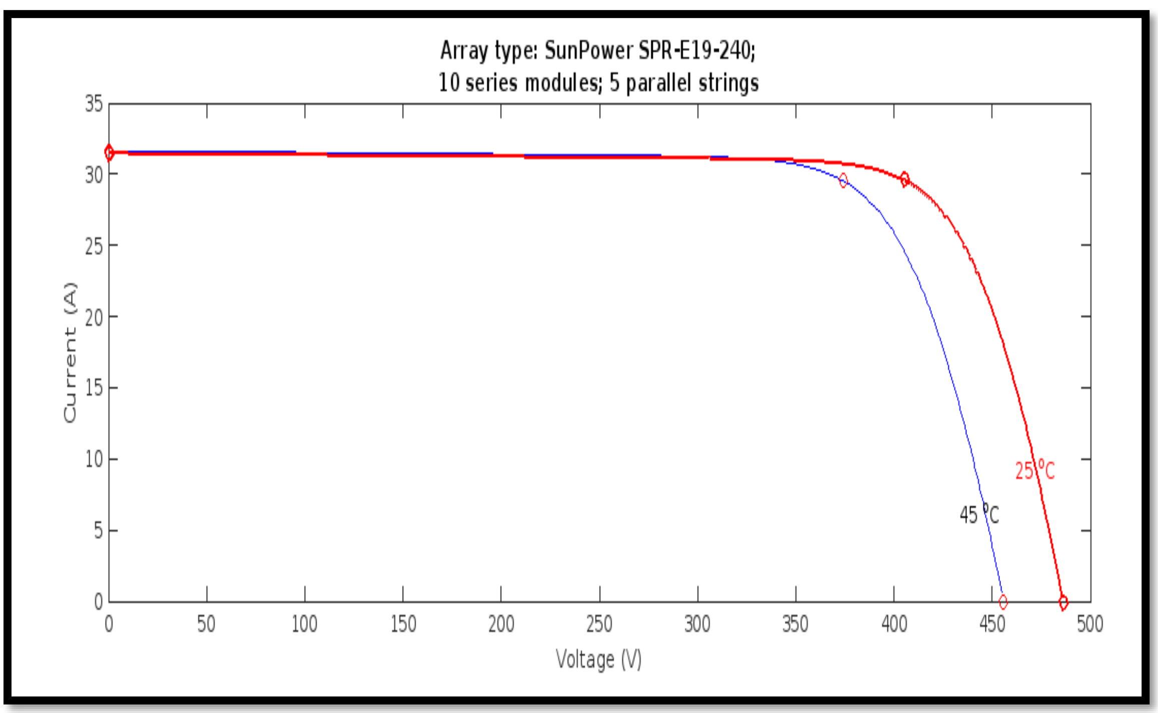

Figure 4.2 PV solar I-V characteristics

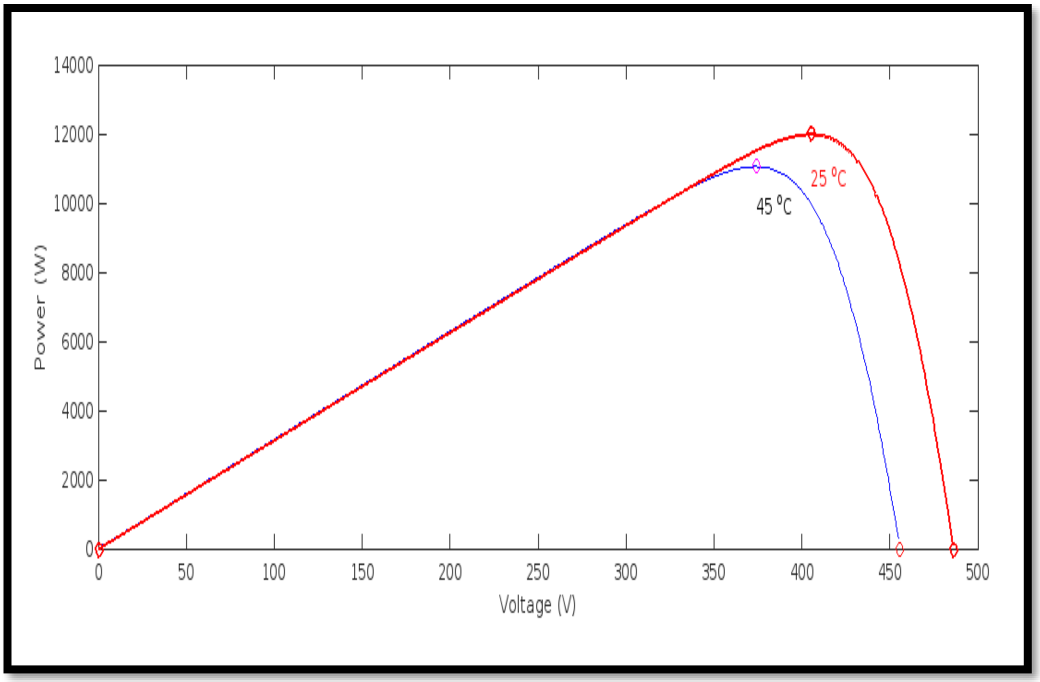

Figure 4.3 PV solar P-V characteristics

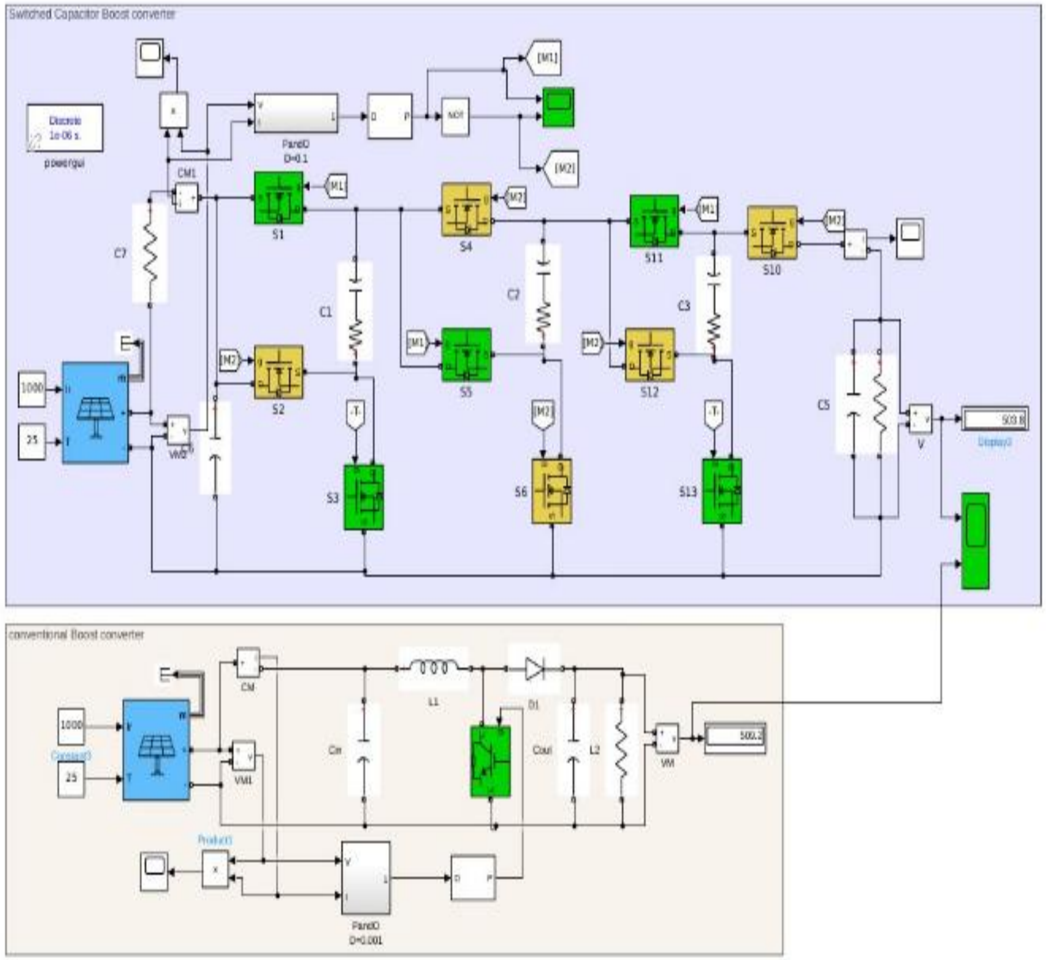

Figure 4.4 Diagrams for SC boost converter and conventional boost converter.

Fig. 4.4 depicts the MATLAB/Simulink block diagram for the two boost configurations, conventional, and the switched capacitor Fibonacci boost converter. The system parameters values are tabulated in Table 4.1. This table includes the whole parameters for the two boost converter configurations and for all MPP technologies.

symbol	Definition	value
PV solar (switched capacitor Boost)		
N_P	parallel strings	3
N_S	series connected modules per string	3
C1,C2,C3,C4,C5	Capacitors	20 μF
C6	Capacitors	100 μF
R1	Input resistance	0.1Ω
R_L	Load resistance	130Ω
PV solar (conventional Boost)		
N_P	parallel strings	7
N_S	series connected modules per string	6
Cin,Cout	Capacitors	1000,100μF
L_1	Inductance	0.9mH
R_L	Load resistance	50Ω
PSO parameters (for switched capacitor boost converter)		
w	Weight	0.79
c1	Constant	1.725
c2	Constant	1.725
PSO parameters (for conventional boost converter)		
w	Weight	0.7
c1	Constant	1.025
c2	Constant	1.025
GA parameters (for switched capacitor boost converter)		
Population Size	Constant	50
Mutation Rate	Constant	0.01
GA parameters (for conventional boost converter)		
Population Size	Constant	100
Mutation Rate	Constant	0.001

Table 4.1 System Parameters.

There are some factors taken into consideration to implement the boost converter with solar PV source. The desired output voltage is defined with respect to the load application, and it is maintained at a constant. These values are dependent on the converter parameters values. However, the input voltage is inconsistent during the comparison. The output voltage of the two boost configurations is compared regarding accuracy, stability, and regulation. Though the voltage ripple, the settling time of the voltage performance has been addressed in the comparison.

In the other hand, the comparison also addresses the output current handling capability of the two boost configurations. It is important to consider that the expected required load current is typically lower than the input current, owing to power conservation principles in boosting converters. However, it is worth noting that if the load current is higher than the converter current capability, a voltage drops or damage to the converter will occur. This poses a challenge in designing a converter that can adequately meet the load requirements of a microgrid.

4.1 Comparative Analysis: Boost vs. FSC Converters

4.1.1 Efficiency and Voltage Regulation under Varying Irradiance

Both the boost and Fibonacci SC converters exhibit different responses to fluctuating irradiance conditions. The conventional boost converter, with its inductor-based design, experiences significant losses due to energy dissipation in the magnetic components. In contrast, the Fibonacci SC converter shows superior voltage regulation and reduced energy losses, particularly under rapidly changing irradiance levels. Studies have shown that SC converters, by eliminating inductors, provide more stable output voltages in dynamic environments.

4.1.2 Power Loss and Heat Dissipation Analysis

Power loss in converters is a critical factor in solar PV systems, as it directly affects efficiency. The conventional boost converter suffers from significant power losses due to inductor and switching losses, which in turn lead to heat dissipation [8]demonstrated that the Fibonacci SC converter has significantly lower power losses compared to conventional designs, as it reduces switching losses and avoids inductor-related losses.

4.1.3 System Stability with Dynamic MPPT Enhancements

System stability is a critical metric in solar PV applications, particularly under dynamic MPPT conditions. The Fibonacci SC converter exhibits better stability compared to the boost converter due to its inherent ability to handle large current variations with minimal voltage fluctuations. The use of advanced MPPT algorithms such as PSO and GA further enhances the stability of the SC converter, ensuring consistent power output even under varying environmental conditions.

4.2 Case Study I: Boost Converter with Dynamic MPPT

4.2.1 Design and Simulation Setup for the Boost Converter

The boost converter design is modeled using MATLAB/Simulink, with an emphasis on simulating real-world solar PV conditions. The inductor size, capacitor values, and switching frequency are optimized to achieve maximum efficiency. P&O and INC MPPT algorithms are implemented to evaluate tracking performance under steady-state and dynamic conditions.

4.2.2 Performance Analysis under SS and Dynamic Conditions

The performance of the boost converter is analyzed under both steady-state and dynamic conditions. While the converter performs adequately in steady-state conditions, it struggles under rapid changes in irradiance, resulting in slower response times and reduced efficiency. The use of P&O for MPPT further exacerbates these inefficiencies due to its tendency to oscillate around the maximum power point.

The P&O algorithm is commonly used in small scale industrial applications since it does not require the system characteristics. However, it fails to obtain optimal power from renewable energy resources.

4.2.3 MPPT Tracking Speed and Conversion Efficiency

MPPT tracking speed is a critical metric for evaluating the performance of the boost converter. The results show that while the boost converter achieves reasonable efficiency in tracking MPP, its conversion efficiency drops significantly in dynamic environments. The slow tracking speed of the P&O algorithm contributes to this inefficiency, particularly in rapidly changing irradiance conditions. The output voltage for the conventional boost converter (Vcon) is settled down at 0.2 second. Figure 4.4 illustrates the output voltage and output current for both conventional boost converters

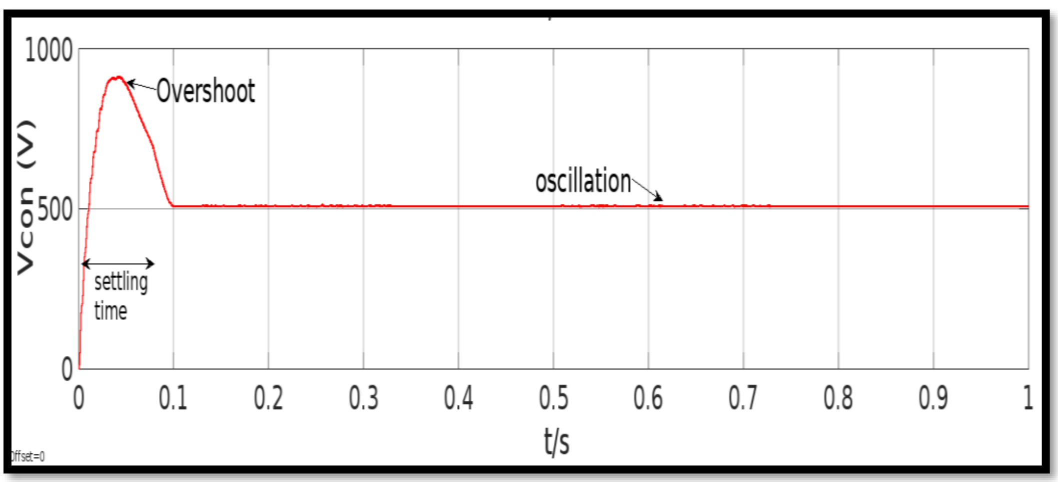

Figure 4.5 Output voltage using P&O MPPT

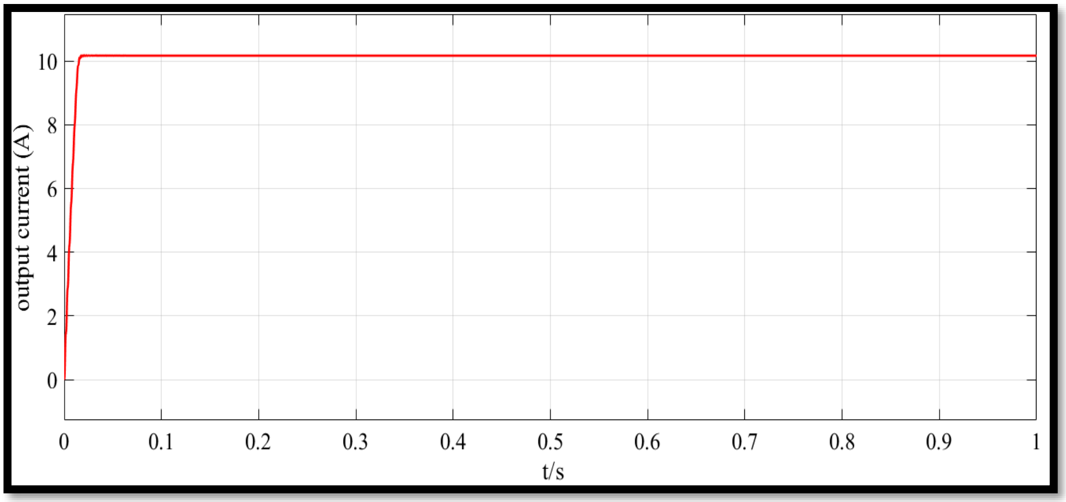

Figure 4.6 Output current using P&O MPPT

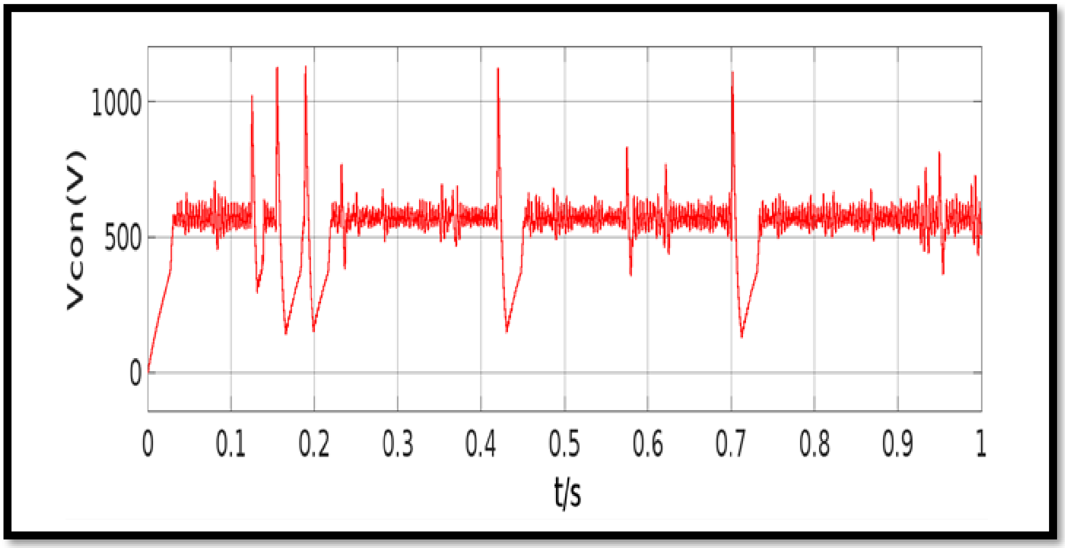

Figure 4.7 **O**utput voltage using INC MPPT

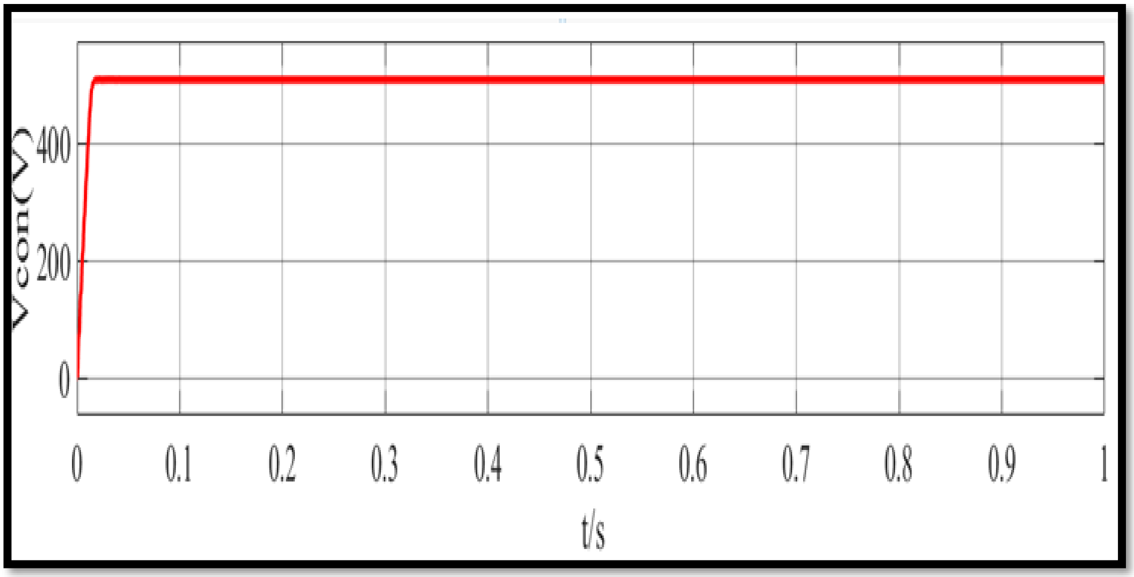

Figure 4.8 Output voltage using PSO MPPT

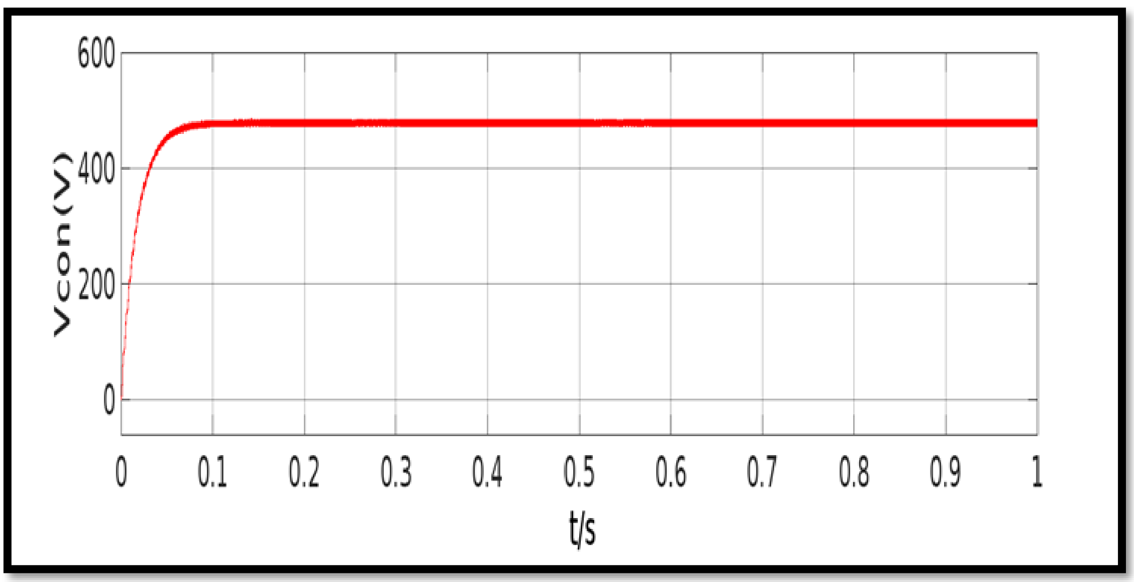

Figure 4.9 Output voltage using GA MPPT

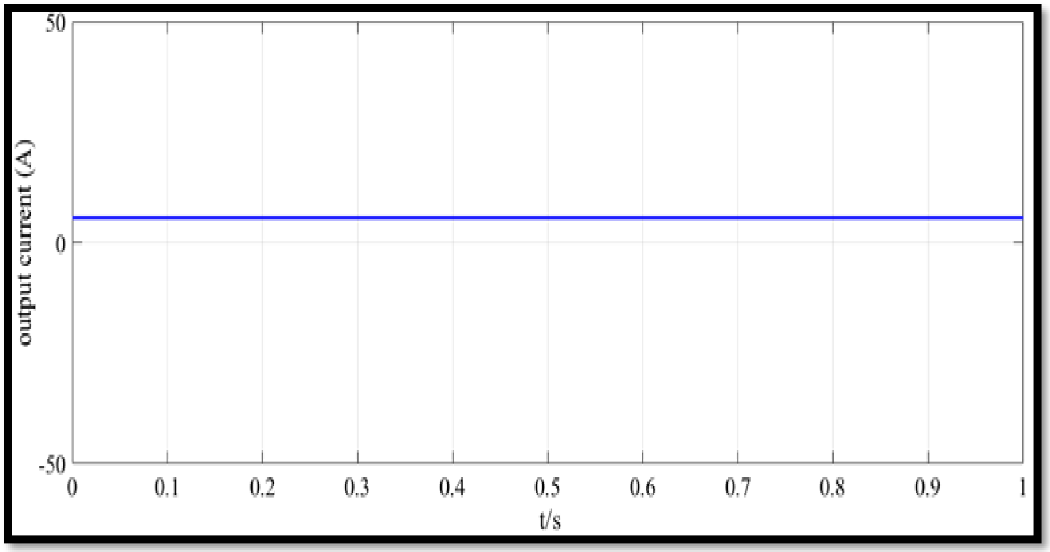

Figure 4.11 Output current using P&O MPPT for SC boost converter

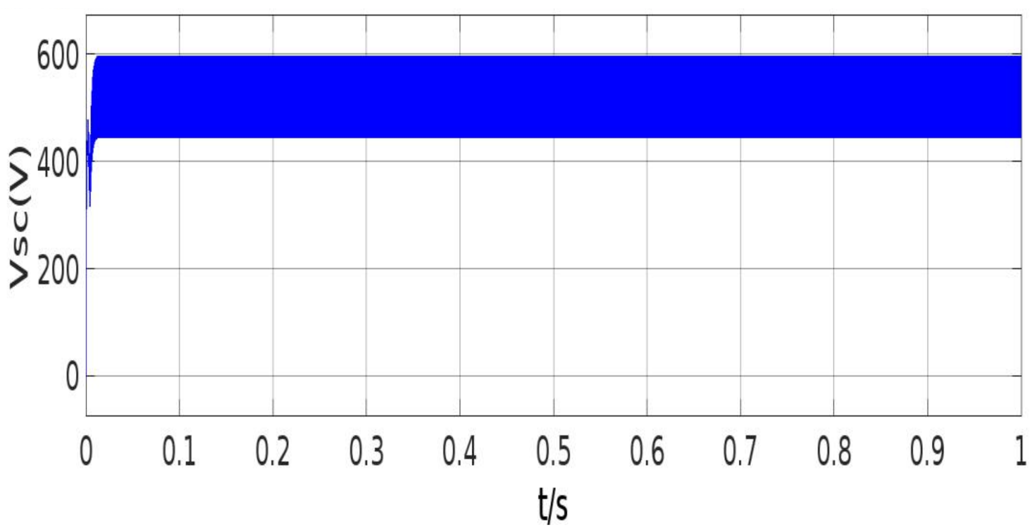

Figure 4.12 Output voltage using INC MPPT for SC boost converter (V_{sc})

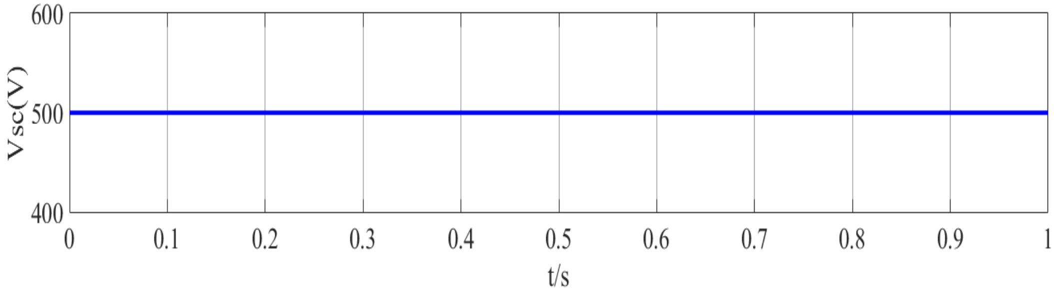

Figure 4.13 Output voltage using PSO MPPT for SC boost converter (V_{sc}).

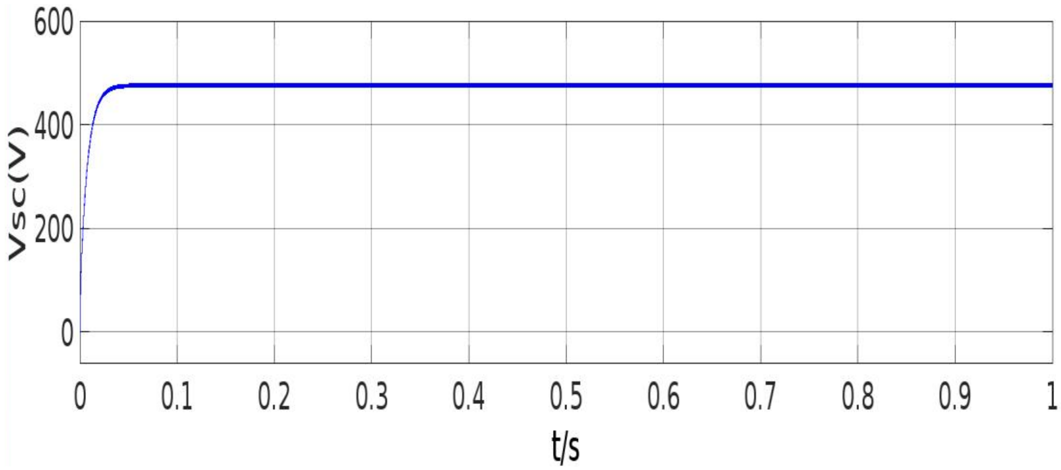

Figure 4.14 Output voltage using GA MPPT for SC boost converter (V_{sc}).

4.3.3 MPPT Tracking Speed and Efficiency with FC

The Fibonacci SC converter demonstrates superior MPPT tracking speed and efficiency compared to the boost converter. The use of PSO and GA allows for rapid convergence to the maximum power point, significantly reducing oscillations and energy losses. Simulation results show that the Fibonacci SC converter outperforms the boost converter in terms of both voltage regulation and power output under dynamic conditions.

4.4 Case Study III: Improved Fibonacci Switched Capacitor Converter

The circuit in figure 3.4 was simulated using MATLAB/SIMULINK under specific operating conditions: an input voltage of 5V, an output voltage of 20V, a switching frequency of 80 kHz, and a load resistance of 500Ω. To enhance the circuit's performance and minimize current spikes, parasitic inductance was incorporated into the design. Figure 4.14 illustrates the input voltage, and the output voltage. The simulation results demonstrate the effective voltage conversion from 5V to 20V, highlighting the circuit's ability to achieve the desired output under the given parameters. The enclosure of parasitic inductance.

plays a crucial role in stabilizing the current flow, thereby improving the overall efficiency and reliability of the system. This simulation provides valuable insights into the circuit's behavior and validates the design's effectiveness in achieving the targeted voltage transformation.

4.4.1: Key performance metrics can be derived from the simulation

- Settling Time: The settling time is the duration it takes for the output voltage to stabilize within a specified range of its final value. In this simulation, the output voltage reaches 20V with minimal overshoot and stabilizes quickly, indicating a well-designed control mechanism. The settling time appears to be relatively short, suggesting that the circuit responds rapidly to changes and maintains stability.

- Ripple Voltage: The output voltage waveform shows a slight ripple, which is typical in switching power supplies. The magnitude of this ripple is crucial as it affects the quality of the output voltage. A smaller ripple indicates better filtering and regulation, which is essential for sensitive electronic components.

- Transient Response: The transient response of the circuit, observed during the initial phase of the simulation, shows how quickly the output voltage rises to its target value. The steep rise in the output voltage waveform suggests an efficient energy transfer and minimal delay in the circuit's response.
- Efficiency: The efficiency of the voltage conversion process can be inferred from the input and output voltage levels. The circuit effectively steps up the voltage from 5V to 20V, indicating a high conversion efficiency. The inclusion of parasitic inductance helps in minimizing current spikes, further enhancing the efficiency by reducing energy losses.
- Stability: The stability of the output voltage is evident from the consistent waveform after the initial transient phase. The absence of significant fluctuations or oscillations in the output voltage indicates a stable and reliable operation.

Overall, the simulation results validate the circuit's design and its ability to achieve the desired voltage transformation with high efficiency and stability. The detailed analysis of settling time, ripple voltage, transient response, and efficiency provides a comprehensive understanding of the circuit's performance, ensuring its suitability for practical applications.

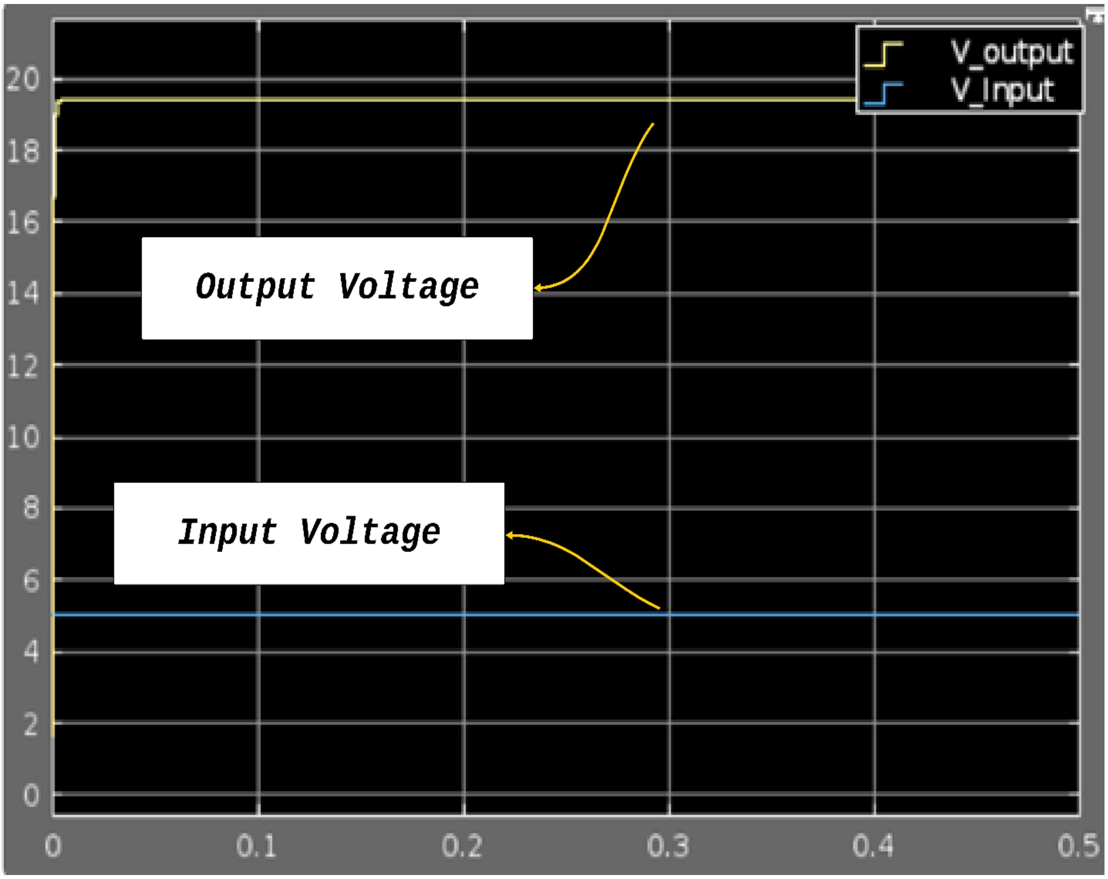

Figure 4.15 Input and Output voltage for Improvement FSC

4.5 Case IV: Hardware Implementation of Improved FSC

The implementation of the Fibonacci switched-capacitor converter presented several challenges, particularly in controlling the MOSFETs within the circuit. Initially, I considered using a microcontroller, such as an Arduino, to manage the switching process. However, after a thorough study of PID controller principles and their application in simulations, I identified a more efficient approach to improve the control mechanism. By analyzing the behavior of the PID controller, I observed that once the system reaches a stable state, the controller no longer requires further adjustments. This insight led me to adopt the CD4007 IC, which generates complementary pulse signals for Phase 1 and Phase 2 switching.

The CD4007 IC plays a critical role in ensuring synchronized switching between the phases, enabling efficient charge transfer and voltage regulation. This approach eliminated the need for a microcontroller, simplifying the design while maintaining precise control over the MOSFETs. The success of this implementation is demonstrated in Figure 4.15

where:

- Channel 1 displays the pulse output from the function generator, which serves as the input to the CD4007 IC.
- Channel 2 shows the complementary pulses generated by the CD4007 IC, which control the MOSFETs for Phase 1 and Phase 2.

The waveforms in Figure 4.15 confirm the proper synchronization of the switching phases, validating the effectiveness of the CD4007 IC in managing the converter's operation. This solution not only addressed the initial challenges but also enhanced the overall efficiency and reliability of the Fibonacci switched-capacitor converter.

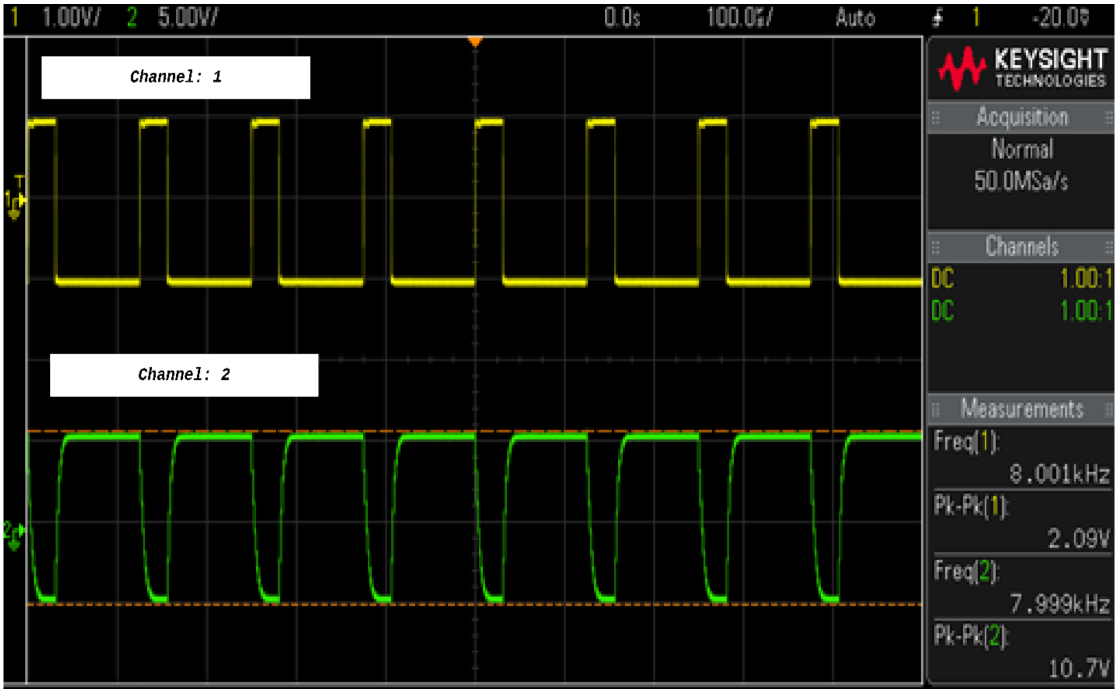

Figure 4.16 Pulse Output from FG and CD4007 IC for Phase Switching

The oscilloscope display in Figure 4.16 provides a detailed analysis of the output voltage of the Fibonacci switched-capacitor converter. The results demonstrate the system's performance under the configured operating conditions. The output voltage waveform shows a stable DC voltage with minimal ripple, indicating effective voltage regulation by the Fibonacci converter. The DC measurement was 18.3V, which confirms that the converter successfully steps up or regulates the input voltage to the desired level.

The waveforms exhibit minimal noise and distortion, reflecting the stability of the system. This stability is achieved through the synchronized operation of the MOSFETs, controlled by the complementary pulse signals generated by the CD4007 IC.

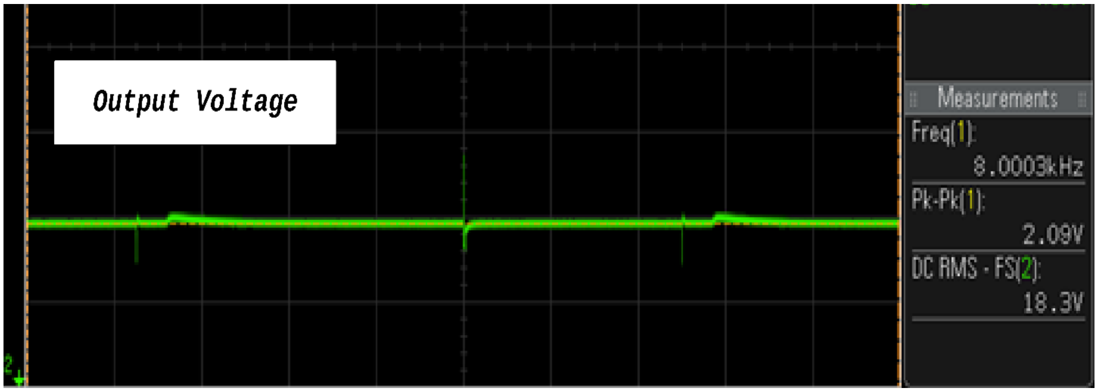

Figure 4.17 Oscilloscope Display of Output Voltage

4.6 The prices of the components used for FSC

Part name	**Price**
Resistors 3 of 3.3K ohms	$ 4.8
Capacitor 4 of 20 μF	$ 0.84
Circuit Breadboard	$ 9.95
Patiki 6 $\times$ 8inch PCB	$ 21.19
MOSFET: IRF 540 N	$ 11.34
Voltage regulator: ELEGCO	$ 1.80
Total cost	$ 49.92

Table 4.2 The price of the components for design Fibonacci Switched Capacitor Converter

4.7 Comparative Performance Evaluation

4.7.1 Analysis of Efficiency, Voltage Regulation, and Power Loss

The comparative analysis reveals that the Fibonacci SC converter outperforms the conventional boost converter in terms of efficiency, voltage regulation, and power loss. The Fibonacci topology's ability to handle high voltage gains without inductors results in lower power losses and improved voltage stability, particularly under dynamic conditions.

The switched capacitor Boost converter utilizes capacitors (C1, C2, C3, C4, C5, and C6) to achieve voltage boosting, while the conventional Boost converter uses inductance (L1) in addition to capacitors (Cin and Cout) for voltage boosting. The switched capacitor Fibonacci boost converter employs capacitors (C1 to C6) with values of 20 μF and 100 μF, while the conventional boost converter uses capacitors (Cin and Cout) with values of 1000 μF and 100 μF, respectively.

4.7.2 Impact of MPPT on System Dynamics: Boost vs. FC

The MPPT algorithms have a significant impact on the system dynamics of both converters. While the conventional boost converter struggles with slow response times and higher oscillations around the MPP, the Fibonacci SC converter, integrated with PSO and GA, demonstrates faster and more stable tracking, leading to better overall system performance.

4.7.3 Practical Implications for Solar PV Integration and CE

The practical implications of these findings are critical for solar PV integration. The Fibonacci SC converter offers a more cost-efficient solution by reducing the need for large inductors and improving system reliability. Moreover, the higher efficiency and better voltage regulation provided by the Fibonacci topology translate into lower energy costs and more reliable solar PV operation.

The simulation results in Table 4.3 show that the switched capacitor boost converter plays an important role in enhancing the MPPT performance. Since the switched capacitor smooths the output voltage and maintains a stable voltage, the conventional converter smooths the current fluctuations. In addition, the GA-MPPT algorithm based on switched capacitor boost converter provides better MPP tracking performance compared with the other MPPT algorithms. The current capability values for each converter based on GA-MPPT are given in Table 4.4.

The switched capacitor has a significantly greater current than that of the conventional converter. According to the values of the current capability, the switches are designed and expected to handle high power applications requirements. Consequently, the comparison between conventional and switched capacitor Fibonacci boost configurations for MPPT methods reveals significant advantages for the switched capacitor configuration. With significantly faster settling times, ranging from less than 1 ms to 0.008 s, and lower output oscillation percentages of 0.02% to 1.02%, the switched capacitor boost configuration outperforms its conventional counterpart across different MPPT methods. This suggests that the switched capacitor Fibonacci boost configuration offers improved performance, stability, and efficiency for maximizing power output in PV solar systems compared to the conventional boost configuration.

Boost Configuration Type	MPPT Method	Settling Time (s)	Output Oscillation %
Conventional	P&O	0.2	0.5
Switched capacitor		0.008	0.02
Conventional	INC	0.05	70
Switched capacitor		0.008	25
Conventional	PSO	0.02	0.8
Switched capacitor		<1 ms	1.02
Conventional	GA	0.04	0.5
Switched capacitor		0.03	0.02

Table 4.3 Simulation results comparison of the output voltage.

The analysis is extended by including additional evaluation data or comparing the GA-based MPPT algorithm with other MPPT techniques. The simulation results for current capability comparison based on the GA-MPPT reveal significant differences between the conventional and switched capacitor Fibonacci boost configurations. The conditions of the GA-based MPPT technique ensure that it adapts to sudden variations in load and solar irradiance, allowing it to effectively optimize the MPPT process over time.

The conventional boost configuration achieves a maximum output current of 10 A; the switched capacitor Fibonacci boost configuration significantly outperforms it, with a maximum output current of 70 A. This indicates that the switched capacitor boost configuration demonstrates a substantially higher current capability, making it more suitable for applications that require greater power output and current handling capacity.

Boost Configuration Type	Maximum Output Current (A)
Conventional	10
Switched capacitor	70

Table 4.4**: C**urrent simulation results comparison based on the GA-MPPT.

In conclusion, for the P&O-MPPT method, the conventional boost configuration exhibits a settling time of 0.2 s with an output oscillation of 0.5%. In contrast, the switched capacitor boost configuration demonstrates a significantly improved performance with a settling time of 0.008 s an output oscillation of 0.02%.

When considering the INC-MPPT method, the conventional boost configuration has a settling time of 0.05 s, with a high output oscillation of 70%. Conversely, the switched capacitor boost configuration displays a superior performance, with a settling time of 0.008 s and a reduced output oscillation of 25%.

For the PSO-MPPT method, the conventional boost configuration achieves a settling time of 0.02 s, with an output oscillation of 0.8%. The switched capacitors boost configuration showcases exceptional speed with a settling time of less than 1 msec and a slightly increased output oscillation of 1.02%.

Under the GA-MPPT method, the conventional boost configuration demonstrates a settling time of 0.04 s with an output oscillation of 0.5%. The switched capacitor boost configuration offers a comparable settling time of 0.03 s and an even lower output oscillation of 0.02%.

Moreover, when examining the current capability simulations based on the GA-MPPT, the conventional boost configuration achieves a maximum output current of 10 A. In contrast, the switched capacitor boost configuration significantly outperforms it, delivering a maximum output current of 70 A.

The switched capacitor configuration demonstrates faster settling times, lower output oscillations, and significantly higher current capability, making it a more promising option for maximizing power output and achieving efficient MPPT in PV solar systems.

Moreover, GA effectively mitigated the negative effects of P&O, INC, and metaheuristic PSO. The GA- MPPT algorithm does not experience any transient oscillations observed in PSO or the steady-state oscillation effects encountered by P&O. Additionally, the GA demonstrates superior robustness compared to other tracking algorithms, particularly in handling inferior regions of the MPP.

4.8 Performance Evaluation of implementation of FSC

The hardwater implementation confirms the successful operation of the Fibonacci switched-capacitor converter. The system achieves stable output voltage regulation with minimal ripple, and the switching waveform demonstrates precise control of the MOSFETs. These results validate the design and implementation of the converter, highlighting its efficiency and reliability in practical applications.

CHAPTER FIVE

FUTURE WORK AND CONCLUSION

5.1 Conclusion

In conclusion, this dissertation has demonstrated that the Fibonacci switched capacitor converter offers significant advantages over the conventional boost converter in solar PV applications. When combined with advanced MPPT algorithms like PSO and GA, the Fibonacci SC converter achieves higher efficiency, better voltage regulation, and faster MPPT tracking speeds, making it a highly effective solution for modern solar PV systems. The simulation results improvement FSC validate the circuit's design and its ability to achieve the desired voltage transformation with high efficiency and stability. Furthermore, hardware implementation of the Fibonacci SC converter could provide validation of the simulation results and explore the real-world performance of this novel topology. The system achieves stable output voltage regulation with minimal ripple, and the switching waveform demonstrates precise control of the MOSFETs. The findings highlight the potential of SC topologies to drive future innovations in solar energy conversion.

5.2 Future Work

Future research should investigate the integration of additional metaheuristic algorithms, such as Artificial Neural Networks (ANNs), with switched-capacitor topologies to further enhance Maximum Power Point Tracking (MPPT) performance. Additionally, there is potential to optimize circuit designs by reconfiguring the conventional boost converter, replacing the inductor with the Fibonacci switched-capacitor topology. This approach could improve overall efficiency and system performance. Further exploration could also involve implementing alternative control methodologies to refine the operation of the converter, enabling better adaptation to dynamic conditions and enhancing its reliability across various applications.

REFERENCES

1. Panagoda, L., et al., *Advancements In Photovoltaic (Pv) Technology for Solar Energy Generation.* Journal of Research Technology & Engineering, 2023. **4**(30): p. 30-72.

2. Saxena, A., et al., *Maximum power extraction from solar PV systems using intelligent based soft computing strategies: A critical review and comprehensive performance analysis.* Heliyon, 2024. **10**(2).

3. Gopi, R.R. and S. Sreejith, *Converter topologies in photovoltaic applications–A review.* Renewable and Sustainable Energy Reviews, 2018. **94**: p. 1-14.

4. Kamarzaman, N.A. and C.W. Tan, *A comprehensive review of maximum power point tracking algorithms for photovoltaic systems.* Renewable and Sustainable Energy Reviews, 2014. **37**: p. 585-598.

5. Singh, G.K., *Solar power generation by PV (photovoltaic) technology: A review.* Energy, 2013. **53**: p. 1-13.

6. Hossain, M. and N. Rahim, *Recent progress and development on power DC-DC converter topology, control, design and applications: A review.* Renewable and Sustainable Energy Reviews, 2018. **81**: p. 205-230.

7. Bouchakour, A., et al., *MPPT algorithm based on metaheuristic techniques (PSO & GA) dedicated to improve wind energy water pumping system performance.* Scientific Reports, 2024. **14**(1): p. 17891.

8. Hawsawi, M., et al., *Conventional and Switched Capacitor Boost Converters for Solar PV Integration: Dynamic MPPT Enhancement and Performance Evaluation.* Designs, 2023. **7**(5): p. 114.

9. Lei, Y. and R.C.N. Pilawa-Podgurski, *A general method for analyzing resonant and soft-charging operation of switched-capacitor converters.* IEEE Transactions on Power Electronics, 2014. **30**(10): p. 5650-5664.

10. de Carvalho Madeira, R.F., *Design of a Fully Integrated Power Management Unit with a Multi-Ratio and Multi-Cell Switched-Capacitor DC-DC Converter*. 2012, Universidade NOVA de Lisboa (Portugal).

11. Saini, S., D.S. Saini, and V. Balyan, *Design Considerations for Power-Efficient Fully Integrated 3: 1 Switched Capacitor DC-DC Converter for PV Modules.* Electronics, 2024. **13**(21): p. 4156.

12. Kushnerov, A., *Multiphase fibonacci switched capacitor converters.* IEEE Journal of Emerging and Selected Topics in Power Electronics, 2014. **2**(3): p. 460-465.

13. Wei, K., *Switched-capacitor Featured Integrated Power Circuit Design for Next-generation Power Management*. 2021.

14. Müller, L.K., *Hard-switched switched capacitor converter design.* 2014.

15. Sathyan, S., et al., *ZVS–ZCS high voltage gain integrated boost converter for DC microgrid.* IEEE Transactions on Industrial Electronics, 2016. **63**(11): p. 6898-6908.

16. Wang, K., et al. *A comparative study of switching losses of IGBTs under hard-switching, zero-voltage-switching and zero-current-switching*. in *Proceedings of 1994 Power Electronics Specialist Conference-PESC'94*. 1994. IEEE.

17. Gu, Y. and D. Zhang, *Interleaved boost converter with ripple cancellation network.* IEEE transactions on power electronics, 2012. **28**(8): p. 3860-3869.

18. Imaoka, J., M. Yamamoto, and T. Kawashima, *High-power-density three-phase interleaved boost converter with a novel coupled inductor.* IEEJ Journal of Industry Applications, 2015. **4**(1): p. 20-30.

19. Forouzesh, M., et al., *Step-up DC–DC converters: a comprehensive review of voltage-boosting techniques, topologies, and applications.* IEEE transactions on power electronics, 2017. **32**(12): p. 9143-9178.

20. Faridpak, B., et al., *Improved hybrid switched inductor/switched capacitor DC–DC converters.* IEEE transactions on power electronics, 2020. **36**(3): p. 3053-3062.

21. Hu, X., et al., *An ultrahigh voltage gain hybrid-connected boost converter with ultralow distributed voltage stress.* IEEE Transactions on Power Electronics, 2020. **35**(10): p. 10385-10395.

22. Lewis, N.S., *Research opportunities to advance solar energy utilization.* Science, 2016. **351**(6271): p. aad1920.

23. Basit, M.A., et al., *Limitations, challenges, and solution approaches in grid-connected renewable energy systems.* International Journal of Energy Research, 2020. **44**(6): p. 4132-4162.

24. Hammad, B., et al., *Modeling and analysis of dust and temperature effects on photovoltaic systems' performance and optimal cleaning frequency: Jordan case study.* Renewable and Sustainable Energy Reviews, 2018. **82**: p. 2218-2234.

25. Bernadette, D., et al., *Analysis of shading effects in solar PV system.* Int. J. Sustain. Green Energy, 2021. **10**(2): p. 47-62.

26. Al-Shahri, O.A., et al., *Solar photovoltaic energy optimization methods, challenges and issues: A comprehensive review.* Journal of Cleaner Production, 2021. **284**: p. 125465.

27. Abdel-Rahim, O., et al., *DC integration of residential photovoltaic systems: A survey.* IEEE Access, 2022. **10**: p. 66974-66991.

28. Qian, T., Y. Yang, and W. Zhao, *A boost-type three-port resonant forward converter with flexible power flow path optimization for PV systems.* IEEE Transactions on Circuits and Systems II: Express Briefs, 2022. **70**(1): p. 161-165.

29. Mouselinos, T.P. and E.C. Tatakis, *Investigation of highly efficient five level asymmetrical inverter family with embedded buck-boost converter.* IEEE Access, 2022. **10**: p. 88750-88768.

30. Saafan, A.A., et al., *A new multiport DC-DC converter for DC microgrid applications.* IEEE Transactions on Industry Applications, 2022. **59**(1): p. 601-611.

31. Li, B., et al., *Design and implementation of a high-power DC/DC converter for HVDC interconnections with wide DC voltage range and fault-blocking capability.* IEEE Journal of Emerging and Selected Topics in Power Electronics, 2021. **10**(1): p. 785-799.

32. Scotta, I.C., W. Maidana, and V. Leite, *Overvoltage protection for gridconnected picohydro generation using photovoltaic inverters.* Revista Facultad de Ingeniería Universidad de Antioquia, 2021(99): p. 73-82.

33. Shenoy, P.S., *Improving performance, efficiency, and reliability of dc-dc conversion systems by differential power processing*. 2012: University of Illinois at Urbana-Champaign.

34. Raghavendra, K.V.G., et al., *A comprehensive review of DC–DC converter topologies and modulation strategies with recent advances in solar photovoltaic systems.* electronics, 2019. **9**(1): p. 31.

35. Alshahrani, A., et al., *The technical challenges facing the integration of small-scale and large-scale PV systems into the grid: A critical review.* Electronics, 2019. **8**(12): p. 1443.

36. Islam, R., S.S.H. Rafin, and O.A. Mohammed, *Comprehensive review of power electronic converters in electric vehicle applications.* Forecasting, 2022. **5**(1): p. 22-80.

37. Sadaf, S., et al., *A novel modified switched inductor boost converter with reduced switch voltage stress.* IEEE Transactions on Industrial Electronics, 2020. **68**(2): p. 1275-1289.

38. Lee, F.C. and Q. Li, *High-frequency integrated point-of-load converters: Overview.* IEEE Transactions on Power Electronics, 2013. **28**(9): p. 4127-4136.

39. Venkatramanan, D. and V. John, *Dynamic modeling and analysis of buck converter based solar PV charge controller for improved MPPT performance.* IEEE Transactions on Industry Applications, 2019. **55**(6): p. 6234-6246.

40. Butzen, N. and M. Steyaert, *Advanced Multiphasing Switched-Capacitor DC-DC Converters*. 2020: Springer.

41. Fettah, K., et al., *Optimal integration of photovoltaic sources and capacitor banks considering irradiance, temperature, and load changes in electric distribution system.* Scientific Reports, 2025. **15**(1): p. 2670.

42. de Souza, A.F., F.L. Tofoli, and E.R. Ribeiro, *Switched capacitor DC-DC converters: A survey on the main topologies, design characteristics, and applications.* Energies, 2021. **14**(8): p. 2231.

43. Smuts, J., *PID controllers explained.* Canadian Process Equipment & Control News, 2002. **2**.

44. Chin, H.H., *All Digital Design and Implementaion of Proportional-Integral-Derivative (PID) Controller.* 2006.

45. Bennett, S., *The past of PID controllers.* Annual reviews in control, 2001. **25**: p. 43-53.

46. Huba, M., et al., *Making the PI and PID controller tuning inspired by Ziegler and Nichols precise and reliable.* Sensors, 2021. **21**(18): p. 6157.

47. Boukenoui, R., et al., *A new intelligent MPPT method for stand-alone photovoltaic systems operating under fast transient variations of shading patterns.* Solar Energy, 2016. **124**: p. 124-142.

48. Sreedhar, S. and D. Jagadeesh, *A review on optimization algorithms for MPPT in solar PV system under partially shaded conditions.* IOSR J. Electr. Electron. Eng, 2016: p. 23-32.

49. Kabalci, E., *Maximum power point tracking (MPPT) algorithms for photovoltaic systems.* Energy Harvesting and Energy Efficiency: Technology, Methods, and Applications, 2017: p. 205-234.

50. Kermadi, M., et al., *Recent developments of MPPT techniques for PV systems under partial shading conditions: a critical review and performance evaluation.* IET Renewable Power Generation, 2020. **14**(17): p. 3401-3417.

51. Ahmad, R., A.F. Murtaza, and H.A. Sher, *Power tracking techniques for efficient operation of photovoltaic array in solar applications–A review.* Renewable and Sustainable Energy Reviews, 2019. **101**: p. 82-102.

52. Verma, D., et al., *Maximum power point tracking (MPPT) techniques: Recapitulation in solar photovoltaic systems.* Renewable and Sustainable Energy Reviews, 2016. **54**: p. 1018-1034.

53. Sarang, S.A., et al., *Maximizing solar power generation through conventional and digital MPPT techniques: a comparative analysis.* Scientific Reports, 2024. **14**(1): p. 8944.

54. Ibrahim, M.H., et al., *Optimizing step-size of perturb & observe and incremental conductance MPPT techniques using PSO for grid-tied PV system.* IEEE access, 2023. **11**: p. 13079-13090.

55. Harrison, A., et al., *An Enhanced P&O MPPT Algorithm for PV Systems with Fast Dynamic and Steady-State Response under Real Irradiance and Temperature Conditions.* International Journal of Photoenergy, 2022. **2022**(1): p. 6009632.

56. Pandey, A., N. Dasgupta, and A.K. Mukerjee, *High-performance algorithms for drift avoidance and fast tracking in solar MPPT system.* IEEE Transactions on Energy conversion, 2008. **23**(2): p. 681-689.

57. Pathak, P.K., A.K. Yadav, and P. Alvi, *Reduced oscillations based perturb and observe solar maximum power point tracking scheme to enhance efficacy and speed of a photovoltaic system.* Journal of Engineering Research, 2023. **11**(2B).

58. Christopher, I.W. and R. Ramesh, *Comparative study of P&O and InC MPPT algorithms.* American Journal of Engineering Research (AJER), 2013. **2**(12): p. 402-408.

59. Mirza, A.F., et al., *Novel MPPT techniques for photovoltaic systems under uniform irradiance and Partial shading.* Solar Energy, 2019. **184**: p. 628-648.

60. Hsieh, G.-C., et al., *Photovoltaic power-increment-aided incremental-conductance MPPT with two-phased tracking.* IEEE Transactions on Power Electronics, 2012. **28**(6): p. 2895-2911.

61. Obukhov, S., et al., *Optimal performance of dynamic particle swarm optimization based maximum power trackers for stand-alone PV system under partial shading conditions.* IEEE Access, 2020. **8**: p. 20770-20785.

62. Ishaque, K., et al., *A direct control based maximum power point tracking method for photovoltaic system under partial shading conditions using particle swarm optimization algorithm.* Applied Energy, 2012. **99**: p. 414-422.

63. Verma, P., et al., *Meta-heuristic optimization techniques used for maximum power point tracking in solar pv system.* Electronics, 2021. **10**(19): p. 2419.

64. Belhachat, F. and C. Larbes, *Comprehensive review on global maximum power point tracking techniques for PV systems subjected to partial shading conditions.* Solar Energy, 2019. **183**: p. 476-500.

65. Zafar, M.H., et al., *A novel meta-heuristic optimization algorithm based MPPT control technique for PV systems under complex partial shading condition.* Sustainable Energy Technologies and Assessments, 2021. **47**: p. 101367.

66. Gad, A.G., *Particle swarm optimization algorithm and its applications: a systematic review.* Archives of computational methods in engineering, 2022. **29**(5): p. 2531-2561.

67. Belhachat, F. and C. Larbes, *A review of global maximum power point tracking techniques of photovoltaic system under partial shading conditions.* Renewable and Sustainable Energy Reviews, 2018. **92**: p. 513-553.

68. Zhang, Y., S. Wang, and G. Ji, *A comprehensive survey on particle swarm optimization algorithm and its applications.* Mathematical problems in engineering, 2015. **2015**(1): p. 931256.

69. Bakht, M.P., et al., *The potential role of hybrid renewable energy system for grid intermittency problem: a techno-economic optimisation and comparative analysis.* Sustainability, 2022. **14**(21): p. 14045.

70. Naseem, M., et al., *Assessment of meta-heuristic and classical methods for GMPPT of PV system.* Transactions on Electrical and Electronic Materials, 2021. **22**: p. 217-234.

71. Othman, P.S., R.R. Ihsan, and R.M. Abdulhakeem, *The Genetic Algorithm (GA) in Relation to Natural Evolution.* Academic Journal of Nawroz University, 2022. **11**(3): p. 243-250.

72. Koutroulis, E., et al., *Methodology for optimal sizing of stand-alone photovoltaic/wind-generator systems using genetic algorithms.* Solar energy, 2006. 80(9): p. 1072-1088.

73. Vannucci, M. and V. Colla, *Fuzzy adaptation of crossover and mutation rates in genetic algorithms based on population performance.* Journal of Intelligent & Fuzzy Systems, 2015. **28**(4): p. 1805-1818.

74. Yap, K.Y., C.R. Sarimuthu, and J.M.-Y. Lim, *Artificial intelligence based MPPT techniques for solar power system: A review.* Journal of Modern Power Systems and Clean Energy, 2020. **8**(6): p. 1043-1059.

75. Senthil Arumugam, M., M. Rao, and A. Chandramohan, *A new and improved version of particle swarm optimization algorithm with global–local best parameters.* Knowledge and Information systems, 2008. **16**: p. 331-357.

76. Tien, J.M., *Internet of things, real-time decision making, and artificial intelligence.* Annals of Data Science, 2017. **4**: p. 149-178.

77. Yoon, D., et al., *An Input-Series Output-Series Noninverting Buck–Boost Converter for 1500 V DC Bus with Wide Input and Output Voltage Ranges.* IEEE Transactions on Industrial Electronics, 2023. **70**(11): p. 11231-11241.

78. Khan, M.S., et al., *Analysis and control of an input-parallel output-series connected buck-boost DC–DC converter for electric vehicle powertrains.* IEEE Transactions on Transportation Electrification, 2022. **9**(2): p. 2015-2025.

79. Alhawsawi, E., et al., *Optimal Design and Operation of Hybrid Renewable Energy Systems for Oakland University. Energies 2023, 16, 5830*. 2023.

80. Chappell, P.H., *Introduction to power electronics*. 2013: Artech House.

81. Law, K., K.E. Cheng, and Y.B. Yeung, *Design and analysis of switched-capacitor-based step-up resonant converters.* IEEE Transactions on Circuits and Systems I: Regular Papers, 2005. 52(5): p. 943-948.

82. Xue, W., et al. *A two-phase hybrid switched capacitors converter with interleaving control scheme for flying capacitors self-balancing*. in *2023 IEEE Applied Power Electronics Conference and Exposition (APEC)*. 2023. IEEE.

83. Sagpazar, N.B., et al. *Three-level resonant switched capacitor Boost converter*. in *2019 10th International Conference on Power Electronics and ECCE Asia (ICPE 2019-ECCE Asia)*. 2019. IEEE.

84. Evzelman, M. and S. Ben-Yaakov. *The effect of switching transitions on switched capacitor converters losses*. in *2012 IEEE 27th Convention of Electrical and Electronics Engineers in Israel*. 2012. IEEE.

85. Thota, P.R. and S. Jeevananthan. *A New Switched Capacitor Nine-Level Inverter with Quadruple Voltage Boosting and Capacitor Voltage Balancing Capabilities*. in *2020 IEEE International Conference on Power Electronics, Drives and Energy Systems (PEDES)*. 2020. IEEE.

86. SinghNeti, S. and V. Singh. *A reduce device count nine level mli using switched capacitors*. in *2020 First International Conference on Power, Control and Computing Technologies (ICPC2T)*. 2020. IEEE.

87. Midya, P. *Efficiency analysis of switched capacitor doubler*. in *Proceedings of the 39th Midwest Symposium on Circuits and Systems*. 1996. IEEE.

88. Cataldo, G.D. and G. Palumbo, *Double and triple charge pump for power IC: Dynamic models which take parasitic effects into account.* IEEE Transactions on Circuits and Systems I: Fundamental Theory and Applications, 1993. **40**(2): p. 92-101.

89. Mahnashi, Y. and F.Z. Peng, *Generalization of the fundamental limit theory in a switched-capacitor converter.* IEEE Transactions on Power Electronics, 2017. **32**(9): p. 6673-6676.

90. Liu, J. and S. Gregori, *Switched-capacitor boost-buck ladder converters with extended voltage range in standard CMOS.* IEEE Transactions on Circuits and Systems I: Regular Papers, 2020. **67**(12): p. 4593-4606.

91. Yi, F. and F. Wang, *Review of voltage-bucking/boosting techniques, topologies, and applications.* Energies, 2023. **16**(2): p. 842.

92. Tanzawa, T. and T. Tanaka, *A dynamic analysis of the Dickson charge pump circuit.* IEEE Journal of solid-state circuits, 1997. **32**(8): p. 1231-1240.

93. Zheng, L., R.P. Kandula, and D. Divan, *Soft-switching solid-state transformer with reduced conduction loss.* IEEE Transactions on Power Electronics, 2020. **36**(5): p. 5236-5249.

94. Murtaza, A.F., et al., *Efficient mpp tracking of photovoltaic (pv) array through modified boost converter with simple smc voltage regulator.* IEEE Transactions on Sustainable Energy, 2022. **13**(3): p. 1790-1801.

95. Murtaza, A.F. and H.A. Sher. *A Series Resonant Network based Boost Converter*. in *2023 International Conference on Emerging Power Technologies (ICEPT)*. 2023. IEEE.

96. Lin, H., et al., *High-current drivability Fibonacci charge pump with connect–point–shift enhancement.* IEEE Transactions on Very Large Scale Integration (VLSI) Systems, 2017. **25**(7): p. 2164-2173.

97. Mahnashi, Y. and F.Z. Peng, *A monolithic voltage-scalable Fibonacci switched-capacitor DC–DC converter with intrinsic parasitic charge recycling.* IEEE Transactions on Very Large Scale Integration (VLSI) Systems, 2019. **27**(5): p. 1105-1113.

98. Uno, M., R. Igarashi, and Y. Sato, *Switched capacitor-based PWM-and phase shift-controlled multiport converter with differential power processing capability for standalone photovoltaic systems under partial shading.* IEEE Journal of Emerging and Selected Topics in Power Electronics, 2020. **9**(5): p. 6019-6032.

99. Sundararaman, K., R. Elavarasu, and R. Sivanand. *A Switched Capacitor Hybrid Fibonacci Converter With Reduced Switches for LED Applications*. in *2020 International Conference on Power, Energy, Control and Transmission Systems (ICPECTS)*. 2020. IEEE.

100. Banerjee, S., A. Ghosh, and S. Padmanaban, *Modeling and analysis of complex dynamics for dSPACE controlled closed-loop DC-DC boost converter.* International Transactions on Electrical Energy Systems, 2019. **29**(4): p. e2813.

LIST OF PUBLICATIONS

Journal Papers:

1- M. Hawsawi, H. M. D. Habbi, E. Alhawsawi, M. Yahya, M. A.Zohdy "Conventional and Switched Capacitor Boost Converters for Solar PV Integration: Dynamic MPPT Enhancement and Performance Evaluation," Designs, vol. 7, no. 5, 2023.

2- E. Y. Alhawsawi, H. M. D. Habbi, M. Hawsawi, and M. A. Zohdy, "Optimal Design and Operation of Hybrid Renewable Energy Systems for Oakland University," Energies, 2023.

3- A. Barnawi, M. Zohdy, T. Hawsawi, E. Alhawsawi, M. Hawsawi, J. Alotaibi, and B. Alabkary, "Optimization of Solar System for Rural Electrification in as Suwadirah (Saudi Arabia)," Engineering Technology Open Access Journal, vol. 4, no. 4, 2023.

4- Khaled Salhein, Sabriya Alghennai Salheen, Ahmed M. Annekaa, Mansour Hawsawi,Edrees Yahya Alhawsawi, C. J. Kobus, Mohamed Zohdy " A Comprehensive Review of Geothermal Heat Pump Systems," Processes, Submitted